Two new ophthalmosaurids (Reptilia: Ichthyosauria) from the Agardhfjellet Formation (Upper Jurassic: Volgian/Tithonian), Svalbard, Norway

Patrick S. Druckenmiller, Jørn H. Hurum, Espen M. Knutsen & Hans Arne Nakrem

Druckenmiller, P.S., Hurum, J.H., Knutsen, E.M. & Nakrem, H.A. Two new ophthalmosaurids (Reptilia: Ichthyosauria) from the Agardhfjellet Formation (Upper Jurassic: Volgian/Tithonian), Svalbard, Norway. *Norwegian Journal of Geology,* Vol 92, pp. 311-339. Trondheim 2012, ISSN 029-196X.

Ichthyosaur diversity near the Jurassic-Cretaceous boundary, particularly from high paleolatitudes, is poorly known. Two recently collected specimens of medium- to large-bodied ichthyosaurs from the Slottsmøya Member of the Agardhfjellet, Svalbard, Norway represent two new taxa of ophthalmosaurids. The holotype specimen of *Cryopterygius kristiansenae* gen et sp. nov., PMO 214.578, is a nearly complete and largely articulated skeleton. The specimen consists of a nearly complete skull, the entire presacral and preflexural vertebral series, numerous dorsal ribs and gastralia, an articulated pectoral girdle and nearly complete forelimb, and an articulated left pelvic girdle and hindlimb. The new taxon is diagnosed on a unique suite of features, including a robust and moderately elongate rostrum, a reduced supranarial process, an elongate maxilla that bears a high number of teeth, the absence of a lacrimal-external naris contact, and an anteroposteriorly broad postorbital bar possessing an unidentified element (supratemporal?) that lies posterior to the quadratojugal. *Cryopterygius* has 52 presacral vertebrae, a distinctive forelimb, including a humerus that bears only two facets at its distal end, and an articulated left pelvic girdle and hindlimb, which facilitates the unequivocal orientation of the ophthalmosaurid femur. The holotype specimen of *Palvennia hoybergeti*, SVB 1451, includes a nearly complete skull and fragmented postcranial remains. It is diagnosed on its relatively short rostrum, greatly enlarged orbit, narrow postorbital bar, very large pineal foramen, basioccipital with broad extracondylar area laterally, and a gracile stapedial shaft. The Slottsmøya Lagerstätte is established as one of the most productive horizons for Upper Jurassic ichthyosaurs and considerably expands our knowledge of ophthalmosaurid diversity and distribution in the latest Jurassic.

Patrick S. Druckenmiller, University of Alaska Museum and Department of Geology and Geophysics, University of Alaska Fairbanks, 907 Yukon Dr., Fairbanks, Alaska, 99775, USA (psdruckenmiller@alaska.edu), Jørn H. Hurum, Espen M. Knutsen & Hans Arne Nakrem, University of Oslo Natural History Museum, P.O. Box 1172, Blindern, NO-0318, Oslo, Norway.

Introduction

The fossil record of Mesozoic marine vertebrates from Svalbard, and particularly from the island of Spitsbergen, has largely been limited to descriptions of Triassic ichthyosaurs from the early radiation of the clade (see reviews in McGowan & Motani, 2003; Maisch 2010) and a handful of plesiosaurians from Jurassic-aged sediments of Svalbard (Wiman, 1914; Persson, 1962; Heintz, 1964). In contrast, the occurrence of Jurassic-aged ichthyosaurs has been limited to a single recent report of a fragmentary rostrum attributed to *Brachypterygius* from the vicinity of Janusfjellet (Angst *et al.*, 2010).

Recent work in the Upper Jurassic Slottsmøya Member of the Agardhfjellet Formation (Volgian) has revealed a remarkable new assemblage of ichthyosaurs in terms of number of specimens and morphological diversity. Between the years of 2004 and 2012, researchers from the University of Oslo Natural History Museum excavated several new ichthyosaur skeletons from Spitsbergen. Two new specimens, representing two new ophthalmosaurid genera, were found on the same hillside on the northwest flank of Janusfjellet and are stratigraphically separated by nine metres of section. The first, PMO 214.578, is a large, exceptionally well preserved skeleton and one of the most complete ichthyosaurs known from the Late Jurassic. The other, SVB 1451, is a nearly complete skull and associated postcranial fragments. Both specimens are described below and compared to other ophthalmosaurids. New morphological data from the Svalbard taxa have a significant bearing on recent and ongoing studies concerning the phylogeny and extinction patterns of Late Jurassic ichthyosaurs, particularly across the Jurassic-Cretaceous boundary (Druckenmiller & Maxwell, 2010; Fischer *et al.,* 2011; Maxwell, 2010; Fischer *et al.,* 2012). Their occurrence at high paleolatitudes also provides new evidence regarding their distribution and paleoecology during this time.

Institutional Abbreviations

BNSS	Bournemouth Natural Science Society, UK
NHMUK	Natural History Museum, London, UK
PMO	University of Oslo Natural History Museum (palaeontological collection), Norway
SVB	Svalbard Museum, Longyearbyen, Norway
UW	University of Wyoming, Laramie, USA.

Geological setting

The vast majority of marine reptile finds collected during the 2004-2012 field seasons by the University of Oslo Natural History Museum from Spitsbergen occur in the Slottsmøya Member of the Agardhfjellet Formation (Figure 1; Hurum et al. 2012). The Agardhfjellet Formation comprises part of the Adventdalen Group (Parker, 1976), a thick succession of Middle Jurassic to Lower Cretaceous sedimentary rocks that crops out extensively in central Spitsbergen. The Agardhfjellet Formation is underlain by shallow shelf to marginal marine sandstone and shale of the Wilhelmøya Formation (Kapp Toscana Group). The Rurikfjellet Formation overlies the Agardhfjellet Formation and together makes up the Janusfjellet Subgroup (Parker, 1976), which consists of several hundred metres of organic-rich, clayey and silty sediment.

Four named members are recognised in the Agardhfjellet Formation, of which the Slottsmøya Member is the uppermost (Dypvik *et al.*, 1991a). The Slottsmøya Member conformably overlies the Oppdalsåta Member and is overlain by the Myklegardfjellet Bed (i.e., the base of the Rurikfjellet Formation; Birkemajer, 1980). The Slottsmøya Member, which averages 55 to 60 metres in thickness in the study area, consists of dark-grey to black silty mudstone, often weathering to paper shale, discontinuous silty beds, with local occurrences of red to yellowish sideritic concretions and seep carbonate bodies, as well as siderite and dolomite interbeds (Dypvik *et al.,* 1991a; Hammer *et al.,* 2011; Collignon & Hammer, 2012). The Slottsmøya Member was deposited in an open marine environment under oxygen-deficient conditions (Nagy & Basov, 1998; Dypvik *et al.,* 1991b). Paleogeographic reconstructions for Svalbard during the Kimmeridgian to Valanginian interval place paleoshorelines several hundred kilometres to the north and west (Dypvik *et al.*, 2002).

The Agardhfjellet Formation ranges from the Middle Jurassic to the Lower Cretaceous based on macrofossils (mostly ammonites: Parker, 1976; Ershova, 1983; Wierzbowski *et al.,* 2011), foraminifera (Nagy & Basov, 1998) and palynology (Løfaldli & Thusu, 1976; Bjærke, 1978). The Slottsmøya Member is largely Volgian (Tithonian) in age, but recent work in the study area indicates that the unit becomes condensed up-section, with the top of the member lying at or close to the Volgian-Ryazanian boundary (Nagy & Basov, 1998; Hammer *et al.,* 2011), or as young as the Boreal Valanginian (Collignon & Hammer, 2012). The specimens described here, PMO 214.578 and SVB 1451, occur in either the *Dorsoplanites maximus* or the *D. ilovaiskyi* zone, corresponding to the Middle Volgian. Precise age correlations between Upper Jurassic and Lower Cretaceous units of the Boreal and Tethyan regions remain controversial (Ogg, 2004; Hammer *et al.,* 2011; Gradstein *et al.,* in press). However, the Middle Volgian age assigned to PMO 214.578 accords with an informally defined Middle Tithonian or Early Portlandian age of the Tethyan region (Gradstein *et al.,* 2012).

To further quantify the stratigraphic occurrence of the vertebrate remains, a laterally continuous, sideritic

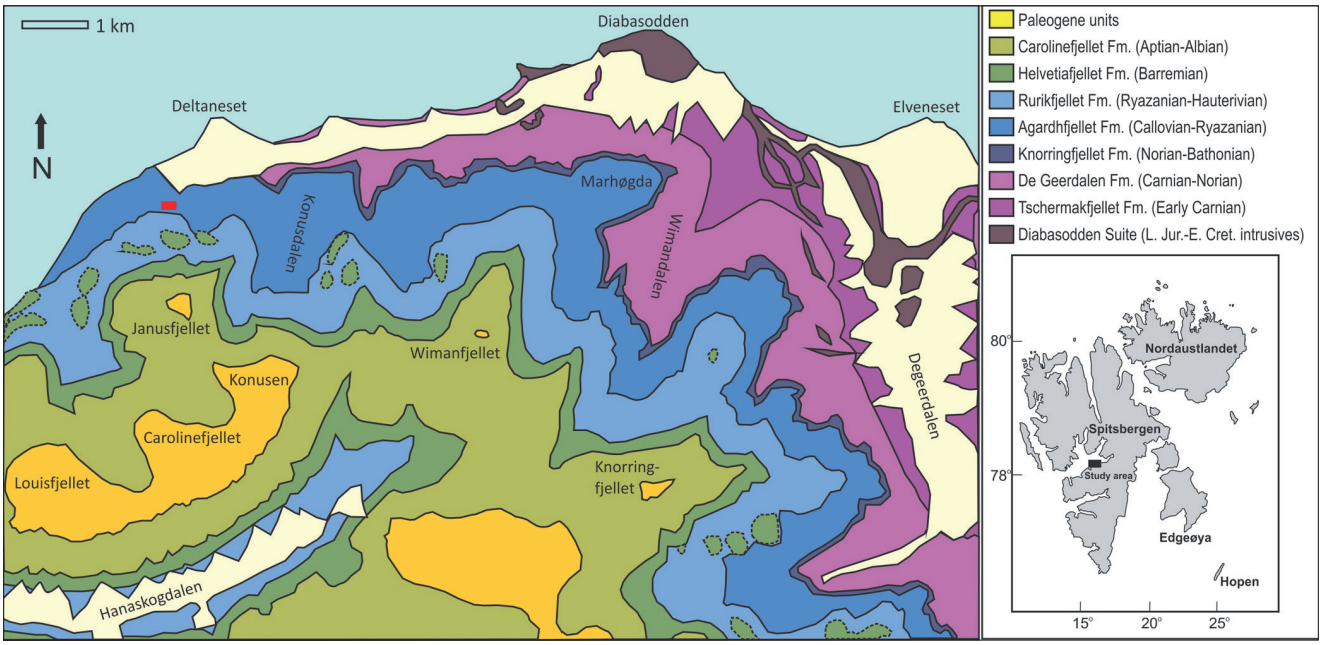

Figure 1. Study area map showing the regional geology and discovery site of PMO 214.578 and SVB 1451 (red mark) in central Spitsbergen, Svalbard, Norway. Both specimens occur in the Slottsmøya Member of the Agardhfjellet Formation, which is Volgian/Tithonian (latest Jurassic) in age. Modified from Dallmann et al. (2001).

horizon rich in ammonites (especially *Dorsoplanites* spp.) and bivalves and a similarly continuous yellow silt bed were used as marker beds against which the stratigraphic position of each skeleton was measured. The yellow silt bed was set at 0 m. The *Dorsoplanites* marker bed occurs 27 m above this yellow layer and 21 m below the top of the Slottsmøya Member (Myklegardfjellet Bed; see Hammer *et al.*, 2011), and occurs in the Middle Volgian *D. maximus* or *D. ilovaiskyi* zone. The vertical position of each vertebrate specimen was recorded with a Leica TCR 110 total station with <1 cm error at 100 metre distance and later corrected with respect to dip. PMO 214.578 was found at 6.2 metres and SVB 1451 15.2 metres below the *Dorsoplanites* bed.

Materials and Methods

PMO 214.578 was removed from the field in 2009 in five major jackets comprising the skull, much of the torso, the forefin, the pelvic girdle and tail. The right side of the specimen was exposed during excavation, but the better preserved left side was mechanically prepared in the laboratory using small picks and brushes, from which the observations and description in this report are largely based. SVB 1451 was excavated in 2004 and the skull was removed in a single jacket. For both specimens, some of the individual bones were also chemically prepared using a solution of sodium chloride to remove a thin layer of gypsum that covers most bones (Charola *et al.*, 2007). After preparation, the specimens were surface-scanned with a three-dimensional laser scanner (Figure 2).

Systematic Paleontology

ICHTHYOSAURIA de Blainville, 1835
OPHTHALMOSAURIDAE Baur, 1887

Genus *Cryopterygius* gen. nov.

urn:lsid:zoobank.org:act:A0F8DD30-2DA6-4D11-96C8-34CAD003B850
Type and only species – C*ryopterygius kristiansenae* sp. nov.
Type locality – North side of Janusfjellet, approximately 13 km northeast of Longyearbyen, Spitsbergen, Svalbard, Norway. UTM WGS84 33N 0518842 8696067.
Type horizon and age – Slottsmøya Member, Agardhfjellet Formation, Middle Volgian, Late Jurassic; 6.2 metres below the *Dorsoplanites* bed within the *Dorsoplanites ilovaiskyi* to *D. maximus* zones (Nagy & Basov, 1998; Collingnon & Hammer, 2012; Gradstein *et al.,* 2012).

Etymology – From *cryo-* (Gr.) meaning cold or frozen and *–pterygius* (Gr.) meaning fin, in reference to its distinctive paddle morphology and its occurrence in high latitudes and excavation out of permafrost.
Diagnosis – as for species.

Cryopterygius kristiansenae sp. nov.
(Figures 2-11)

urn:lsid:zoobank.org:act:40BEB21D-3CFF-4D4B-A9D3-B2EA7AFC6575
Holotype – PMO 214.578, a nearly complete skull, the entire presacral and preflexural vertebral column,

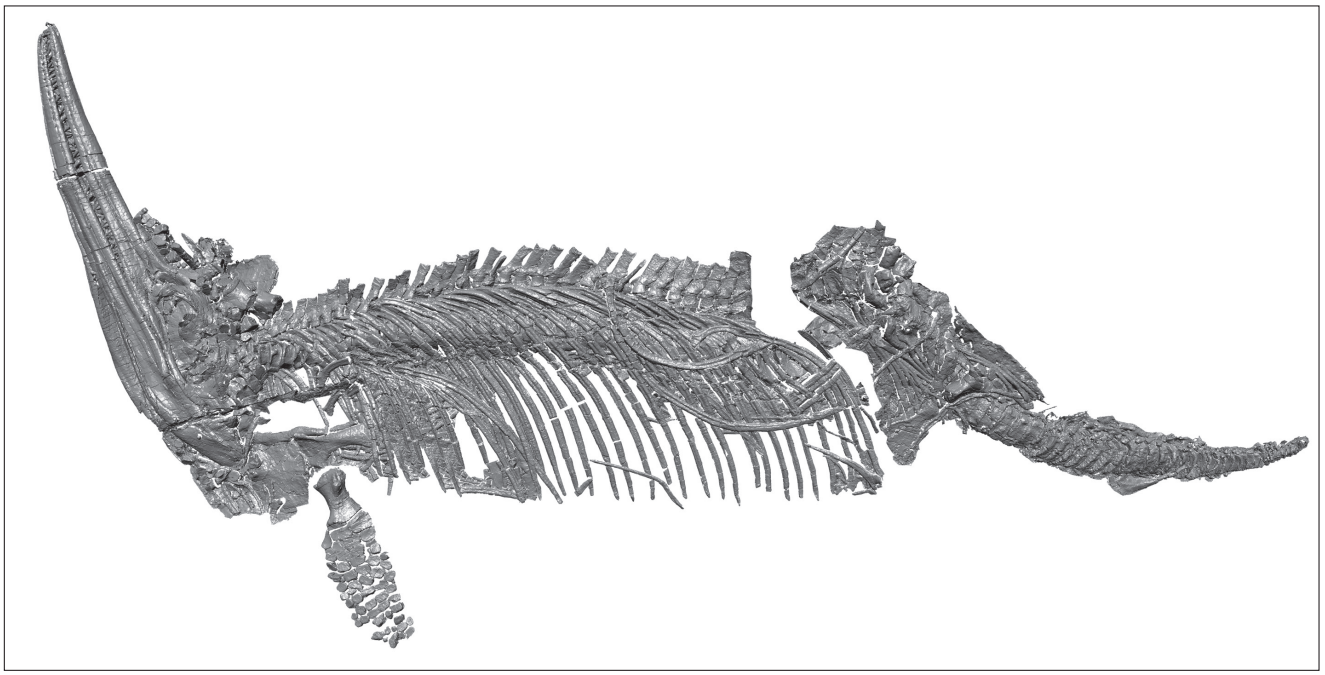

Figure 2. Surface laser scan of the holotype specimen of Cryopterygius kristiansenae, *PMO 214.578 from the Slottsmøya Member, Agardhfjellet Formation, Spitsbergen, Svalbard, Norway. Skeleton as preserved is 4.6 metres in length.*

numerous ribs and gastralia, most of the right and left pectoral girdle and limb, and the left pelvic girdle and hind limb.

Etymology – *kristiansenae*, in honour of Lena Kristiansen, long-time participant in the Spitsbergen Jurassic Research Group fieldwork on Spitsbergen.

Differential diagnosis – large ophthalmosaurid ichthyosaur (estimated 5.5 metres total body length) with the following autapomorphies and unique character combinations: robust rostrum with snout ratio of 0.61 (relatively longer and more gracile in *Aegirosaurus, Nannopterygius*); orbital ratio of 0.19 (relatively larger in *Ophthalmosaurus, Nannopterygius*); supranarial process of premaxilla strongly reduced and not contacting the external naris (well developed supranarial process contacting the external naris in *Brachypterygius* and *Caypullisaurus*); subnarial process does not contact the jugal (contacts jugal in *Brachypterygius*); lacrimal does not contact the external naris (contacts external naris in *Ophthalmosaurus*, *Caypullisaurus*, *Aegirosaurus*, *Sveltonectes*); posterior margin of lacrimal forms distinct, nearly 90 degree angle (autapomorphic); maxilla with 23 teeth (10-13 in *Ophthalmosaurus*); maxilla with extensive lateral exposure along the toothrow, extending as far posteriorly as the midpoint of the orbit (shorter exposure laterally in *Brachypterygius*, *Aegirosaurus*, *Ophthalmosaurus*); jugal nearly straight (bowed in *Aegirosaurus*, *Ophthalmosaurus*); postorbital bar anteroposteriorly broad (narrow in *Ophthalmosaurus*, *Aegirosaurus*, *Nannopterygius*); element (supratemporal?) located posterior to the quadratojugal with a narrow, ventrally projecting process (autapomorphic); 53 teeth in upper toothrow (premaxilla and maxilla; 40 in *Ophthalmosaurus*); teeth relatively robust and large with numerous, fine, enamelled ridges (relatively smaller and more gracile in *Aegirosaurus* and *Sveltonectes*); 52 presacral vertebrae (42-43 in *Ophthalmosaurus*, 37(?) in *Platypterygius americanus*); conspicuous V-shaped notch along the dorsal margin of presacral neural spines as seen in lateral view (autapomorphic among ophthalmosaurids); ribs 8-shaped in cross section (round in *Acamptonectes*); relatively small forelimb bearing 5-6 digits (relatively larger with 6+ digits in *Caypullisaurus*, *Platypterygius*); humerus with two distal facets only (three facets in *Ophthalmosaurus*, *Aegirosaurus*, *Caypullisaurus*, *Undorosaurus*, *Brachypterygius*, *Arthropterygius*, *Acamptonectes*); rounded phalanges (rectangular in *Platypterygius*, *Sveltonectes*); ischiopubis expanded and unfused distally (unlike *Ophthalmosaurus*); femur anteroposteriorly broad with two facets distally (three distal facets in *Platypterygius americanus*, *P. australis*).

Description

The holotype skeleton, PMO 214.578, measures 4.6 m in length as preserved (Figure 2). The skeleton is nearly complete and largely articulated, although the right forelimb has been displaced and disarticulated, and the right pelvic girdle and the postflexural region of the tail is missing. The carcass came to rest on the sea floor on its left side; as a result, some of the elements on the right side (stratigraphically up) have been either been displaced, damaged or altogether lost. In contrast, the left side of the skeleton is very well preserved, is largely articulated, and lacks the surface damage found in some elements, such as the vertebral centra (see below), on the right side. A number of small faults with less than 10 cm of displacement cross-cut the specimen and many of the bones are highly fragmented, likely due to congelifraction. The skeleton was collected in five major blocks, including the anterior half of the rostrum, the skull and pectoral girdle, the left forelimb, the torso and the pelvic girdle and tail. The better-preserved left side of the skeleton was prepared in the laboratory and it is from this side that most elements are described.

The specimen is interpreted to be an adult. Although the postflexural vertebrae are missing, the animal had an estimated total length of 5.0 to 5.5 m, which is relatively large compared to other Late Jurassic ichthyosaurs (Fernández, 1997; Bardet & Fernández, 2000). Using the ontogenetic criteria of Johnson (1977), the proximal articular surface of the humerus and femur are prominently convex, the surface of the humeral shaft is relatively smooth, and there is considerable closure between the joint surfaces in the proximal fin elements of the forelimb, all indicative of an adult ontogenetic stage.

Skull

The entire left surface of the skull is well preserved (Figures 3, 4) in lateral view, as is part of the medial surface of the right lower jaw. The palate is not visible. The dorsal surface of the skull is heavily damaged due to crushing and much of the disarticulated right pectoral girdle and forelimb came to rest in this area. As a result, the morphology of the skull roof, including the temporal fenestrae, the pineal foramen, and most of the dermal elements cannot be interpreted. Portions of the braincase are visible in the left orbit, whilst others, such as the basioccipital, are displaced and are only visible on the right side of the specimen, which is presently unprepared.

The holotype skull of *Cryopterygius* possesses a robust rostrum, with a "snout" ratio (preorbital length/length of lower jaw; McGowan, 1974) of 0.61 and a prenarial ratio (prenarial length/length of lower jaw) of 0.83 (Table 1). The well preserved premaxillae are slightly disarticulated along the midline and contact their opposites for approximately half of the total preorbital length. The premaxillary ratio (Kirton, 1983; length of premaxillary segment (tip of rostrum to posterior point of premaxilla along the toothrow)/snout length) is 0.73. Approximately 30 teeth are visible in the left premaxilla. Conspicuous nutrient foramina are visible dorsal to the toothrow along the lateral margin of the premaxilla; anteriorly each foramen is discrete, but posteriorly the foramina coalesce into

Figure 3. Photograph of the holotype skull of Cryopterygius kristiansenae, *PMO 214.578, in left-lateral view.*

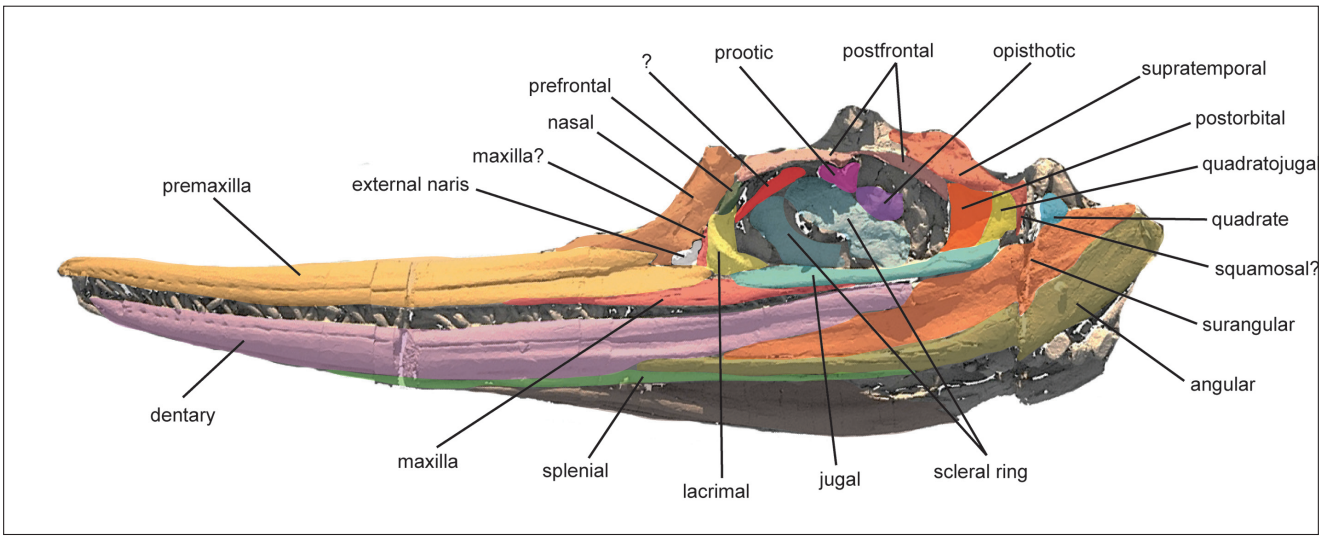

Figure 4. Interpretation of the holotype skull of Cryopterygius kristiansenae, *PMO 214.578, in left-lateral view.*

a single longitudinal groove. At its posterior end, the supranarial process of the premaxilla is reduced and does not contact the anterior border of the external naris (Figure 5). The subnarial process extends further posteriorly, participates in the entire ventral margin of the external naris, and terminates in a short contact with the anteroventral margin of the lacrimal. The premaxilla does not contact the jugal.

In lateral view, the maxilla has considerable exposure along the toothrow (Table 1) representing 38 percent of the total toothrow length and has a maxillary ratio (McGowan, 1974; length of premaxillary segment/length of lower jaw) of 0.27. The maxilla has elongate and tapering contacts with the premaxilla anteriorly, the jugal posteriorly, and it bears a short contact with the lacrimal dorsally. The maxilla terminates posteriorly at

Table 1: Selected cranial measurements of PMO 214.578 (in cm).

Maximum skull length (premaxilla to posterior margin of postorbital bar)	122
Anteroposterior length of orbit	27
Minimum internal diameter of scleral ring	8
Width of lateral surface of scleral plate	5.5
Preorbital (snout) length	85
Length of premaxilla along tooth row	62
Total length of toothrow	100
Anteroposterior length of postorbital bar	9
Maximum length of lower jaw (left ramus)	139

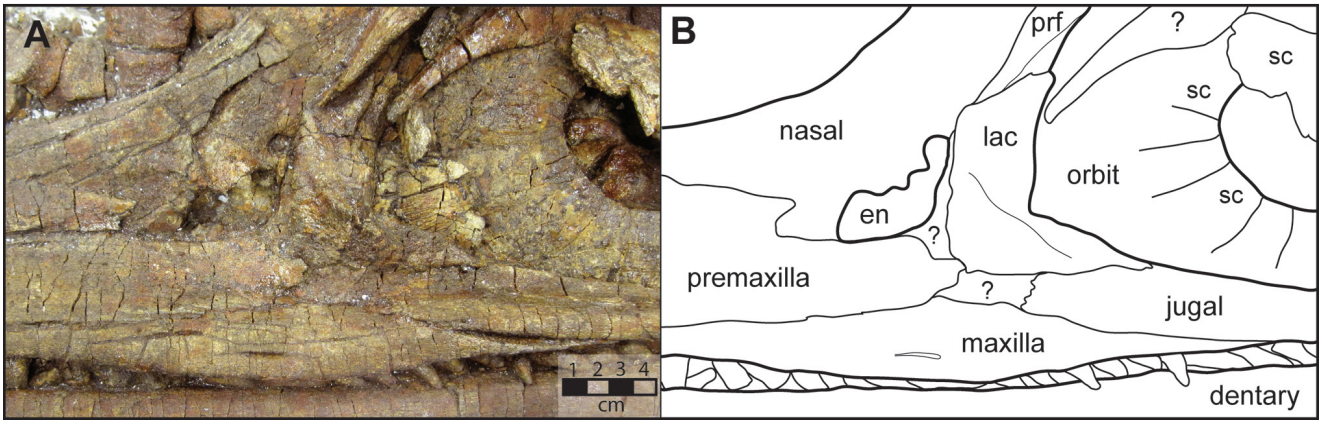

Figure 5. Photo (A) and interpretation (B) of the antorbital region of the skull of the holotype specimen of Cryopterygius kristiansenae, *PMO 214.578, in left-lateral view. Abbreviations: en, exteral naris; lac, lacrimal; prf, prefrontal; sc, scleral plate.*

approximately the midpoint of the orbit. Twenty-three teeth are visible in the maxilla, giving a total of approximately 53 teeth in the upper toothrow. In external view, the tallest dorsoventral height of the maxilla lies in line with the posterior margin of the external naris. Delimiting the dorsal margin of the maxilla is difficult, but it appears that a posterior ascending process of the maxilla is visible between the lacrimal and external naris, and forms the entire posterior margin of the latter. The external naris is anteroposteriorly longer than tall. A secondary embayment of the external naris lies at its posterodorsal margin. An ascending anterior process of the maxilla is not visible, nor is any definitive contact posteriorly with the prefrontal.

The jugal overlaps the maxilla anteriorly and contacts the lacrimal anterodorsally. The jugal is 34 cm long in total length, forms the entire ventral margin of the orbit and is not bowed in shape but rather is nearly straight. Posteriorly, it forms the ventral margin of the postorbital bar and approaches, but does not contact, the descending process of the probable supratemporal (described below).

Because the skull is crushed mediolaterally, the relationships of the nasals to other elements are difficult to interpret. The contact between the left and right nasal is visible but somewhat damaged; although an internasal foramen does not seem present, poor preservation makes its presence or absence equivocal. The relationships between the nasal and the frontal, supratemporal and postfrontal cannot be discerned due to crushing in this area. The nasal appears to share at least a short contact with the lacrimal.

A well preserved lacrimal is present and forms the anteroventral margin of the orbit. However, its posterior margin, which forms the anteroventral border of the orbit, bears a well-defined bend of nearly 90 degrees (Figure 5). The anterior margin of the lacrimal does not contact the external naris, being narrowly separated from it by what is possibly the posterior ascending process of the maxilla. Dorsally, the lacrimal contacts the prefrontal but the exact nature and location of this contact is unclear. It is interpreted here to abut the prefrontal along a broad contact at mid height of the orbit, corresponding to a distinct fold in the bones due to crushing. A prominent ridge slopes obliquely anterodorsally to posteroventrally across the lateral surface of the lacrimal.

The dorsal rim of the orbit is formed by the prefrontal and postfrontal. The prefrontal is interpreted to form only the anterodorsal corner of the orbital rim, although its relationships to the postfrontal are difficult to discern. The size and margins of the postfrontal are interpreted based on bone fibre orientation, which radiates from the middle of the bone and helps distinguish it from neighbouring elements. It is a large element that forms approximately two-thirds of the dorsal border of the orbit. Its degree of contact with the supratemporal medially and the postorbital posteriorly are difficult to interpret due to damage.

The postorbital bar is conspicuously broad anteroposteriorly compared to total skull length and comprises the postorbital, quadratojugal and an unidentified third element (Figure 6). The postorbital forms the entire posterior margin of the orbit and is rectangular in shape, being twice as tall as it is broad at its midpoint. Its relationship to the postfrontal at the posterodorsal margin of the orbit and the supratemporal dorsally is unclear due to damage in the orbital rim. The posterior margin of the postorbital is formed entirely by the quadratojugal, which is also taller than broad. The dorsal and posterior margins of the quadratojugal are bordered by a third element whose identity is equivocal. The posteroventral portion of this unknown element forms a narrow descending bar along the posterior border of the skull. It also bears a short ventrally-projecting process at the extreme posteroventral margin of the skull, forming a small notch

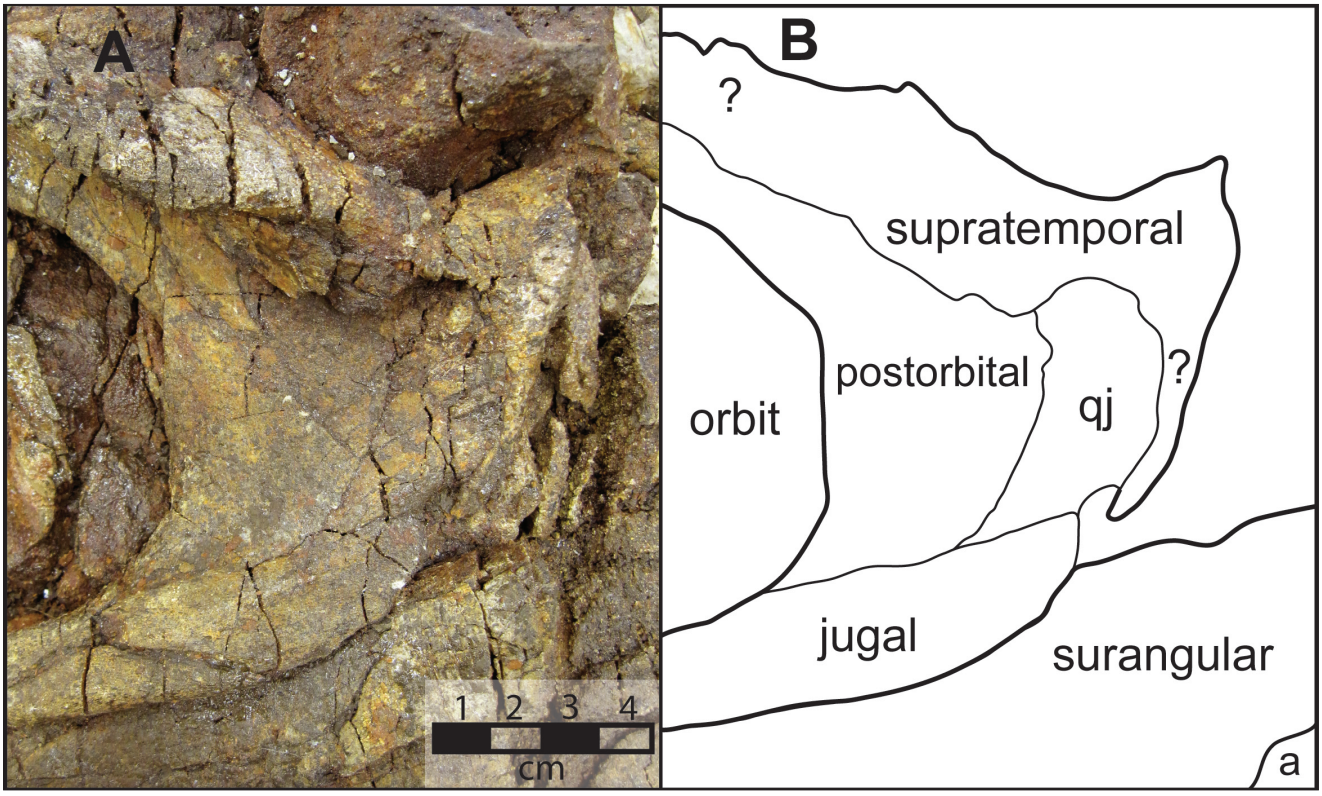

Figure 6. Photo (A) and interpretation (B) of the postorbital region of the skull of the holotype specimen of Cryopterygius kristiansenae*, PMO 214.578, in left-lateral view. Abbreviation: a, angular; qj, quadratojugal.*

along the posterior border of the jugal and quadratojugal. Topologically, this element may be homologous to the ventral process of the supratemporal. Although this region is well preserved, there is no indication of a sutural contact within this element to discern whether it may even be partly composed of a fused supratemporal and squamosal. No clear indications otherwise for a squamosal are present.

The orbit is large (Table 1) and represents 22 percent of total skull length and has an orbital ratio (diameter of orbit/length of lower jaw) of 0.19. The anterior half of the scleral ring is well preserved but the posterior half has been displaced due to crushing. The scleral ring appears to have largely filled the orbit. A number of isolated elements of the braincase are also partially visible in the left orbit, including a prootic, on which impressions for the semicircular canals can be seen, the ventral articular surface of a right quadrate, and an opisthotic. Other elements of the braincase, including the basioccipital, basisphenoid and stapes, are not well exposed on this surface. The basioccipital in particular was observed in the field at the time of collection and adheres to the typical ophthalmosaurid condition of having a reduced extracondylar area, but other details are currently unavailable. Finally, an isolated and elongate bone was found lying in the anterodorsal portion of the orbit. It is 10.5 cm long, has a pointed anterior end, and becomes broader posteriorly, and is narrowly oval in cross section at its midpoint. This may represent a displaced anterior cervical rib or is another unidentified cranial element.

Mandible

The left and right dentaries lie in contact with one another for approximately 0.5 m, or close to half of their total length. Because the left and right rami are crushed together, it is hard to discern exactly where the posterior end of the mandibular symphysis was located. In lateral view of the left ramus, the dentary gradually tapers posteriorly to a point in line with the posterior margin of the orbit, although its exact end is hard to discern. The dentary contacts the splenial and angular ventrally, and overlaps the surangular posteriorly. Similar to the premaxillae, the nutrient foramina parallelling the toothrow are discrete anteriorly, but coalesce into a single groove posteriorly. The total number of dentary teeth is uncertain.

The splenial can be seen to participate in the mandibular symphysis beginning approximately 30 cm from the anterior end of the ramus. From this point the splenial gradually becomes more visible in lateral view along the ventral margin of the jaw, becoming best exposed (as measured in dorsoventral height) around the middle of the ramus where it is bordered anteriorly by the dentary and posteriorly by the angular. The posterior end of the splenial is visible on the medial surface of the right ramus, where it terminates in a forked end that lies approximately in line with the posterior border of the orbit.

Anteriorly and in lateral view, the angular splits the splenial ventrally from the dentary dorsally and then extends posteriorly as a thin wedge of bone along the ventral margin of the mandible. Posteriorly, in the area of the mandibular condyle, the angular abruptly increases in dorsoventral height, lies ventral to and laterally overlaps the surangular, and comprises approximately two-thirds of the total dorsoventral height of the posterior portion of the lower jaw in lateral view.

Anteriorly, the surangular is first visible in lateral view at a point in line with the external naris and then expands in dorsoventral height to occupy approximately the middle third of the lateral surface of the jaw. Posteriorly, the surangular forms the dorsal portion of the ramus and bears small crenulations along its posterodorsal margin. No portion of the articular is visible, being covered entirely by the surangular, but what is interpreted as the distal end of the left quadrate is partially exposed just posterior to the mandibular condyle.

A small portion of the prearticular is visible on the medial surface of the right ramus where it lies dorsal and medial to the splenial, but little else can be said about this element.

Dentition

The enamelled crowns have a maximum crown height of approximately 26 mm, giving a tooth length index (10x maximum crown length of longest tooth/jaw length) of 0.19 (McGowan, 1976). There is little variation in fully developed crown height along the toothrow other than a gradual reduction in size posteriorly. The crowns bear numerous fine, tightly packed, straight enamel ridges on their labial surfaces, and so far as can be discerned, on their lingual surfaces as well. However, near the apices the crowns lack any ornamentation or ridges, even on newly erupted teeth, suggesting this is their true morphology and not simply due to wear. There is no indication of prominent carinae. The teeth have a gentle distal curvature and the crowns are nearly round in cross section.

Axial skeleton

Ninety vertebrae are preserved in the holotype of *Cryopterygius*, most of which remain largely in articulation, although there is a slight displacement in the axial column in the posterior dorsal region. None of the neural arches are fused to the centra, but many remain in articulation with one another, even in the dorsal series, where the arches have been slightly displaced as a unit dorsally from the centra. The preservation of the left and right halves of the vertebral centra varies considerably; the surface texture and morphology of the left (stratigraphically down) side are well preserved whereas on the right (stratigraphically up) side they are often pitted and uneven and structures such as rib facets are not discernible. Most of the dorsal ribs of the right side are either lost or displaced, whilst those on the left remain in life position.

A total of 52 presacral vertebrae are present in *Cryopterygius* measuring 2.2 m in total length. The end of the presacral series was defined solely by its relationship to the ilium, which lies in direct contact against centra 53 and 54. It was not possible to determine whether this corresponds to the point at which the diapophysis and parapophysis coalesce due to taphonomic reasons.

The atlas-axis complex is completely fused and only a low ridge along the lateral face of the complex indicates the sutural boundary. The atlas centrum is slightly longer anteroposteriorly than the axis. A distinct atlas diapophysis and parapophysis cannot be discerned, but a single apophysis, probably the parapophysis, is visible in the dorsal and posterior half of the axis. The presence or absence of an atlantal or axial intercentrum is equivocal, as this area lies within a fault plane and the neural arches are covered by parts of the skull.

Only general observations regarding variation in vertebral dimensions are possible given that the centra are either covered by the dorsal ribs, are tightly articulated, or in some cases are obliquely distorted. For these same reasons, most of the apophyses are also not visible, making it impossible to delimit axial regions such as the end of the cervicals (where the neural arch and diapophysis lose contact) and

Table 2: Selected axial measurements of PMO 214.578 (in mm). Length was measured along the lateral surface of the centrum; height of the neural arch was measured from base of the pedicel at the neurocentral boundary to the midpoint of the spine along the lateral surface.

Centrum number	Length	Neural arch height
1, 2 (atlas/axis)	55	-
4	34	-
7	33	85
14	38	90
16	36	110
29	45	125
35	46	120
40	38	-
44	45	100
49	42	-
57	40	-
61	38	-
65	34	-
71	30	-
76	27	-

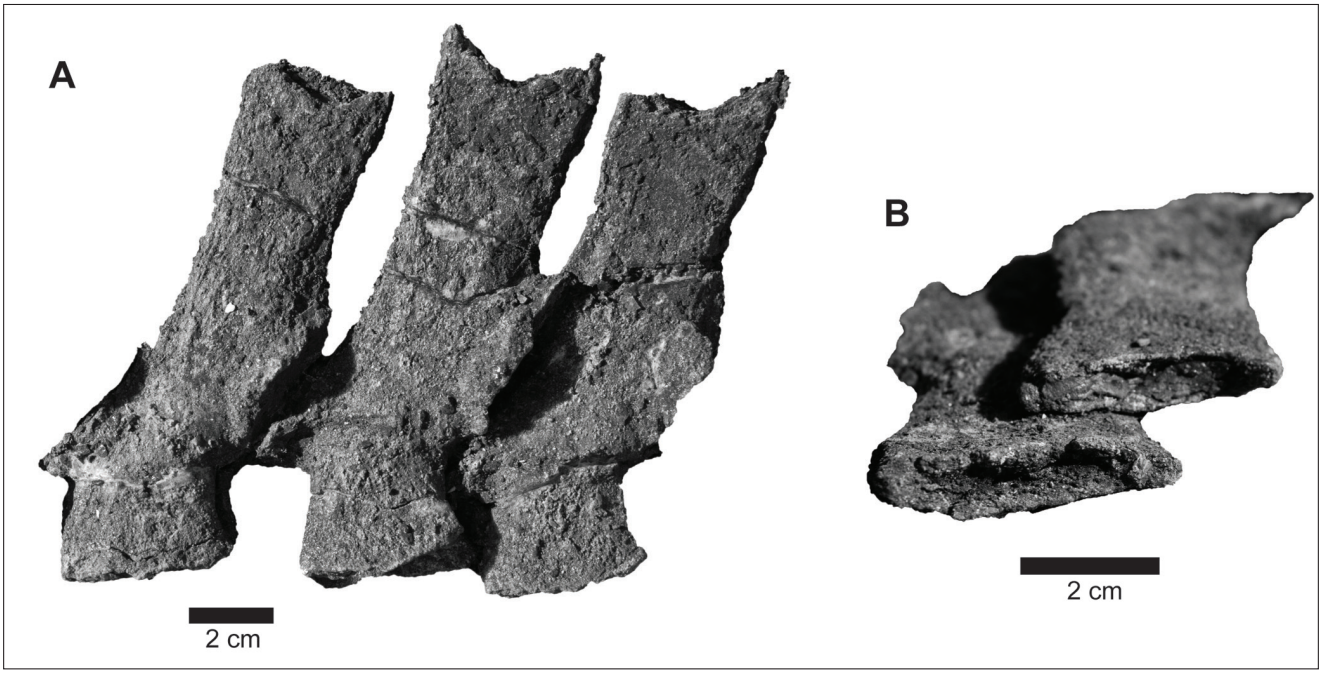

Figure 7. Neural spines from the mid-dorsal region of the holotype specimen of Cryopterygius kristiansenae*, PMO 214.578, in left-lateral (A) and dorsal (B) views.*

the start of the sacral series (see above). Measurements of selected vertebral lengths are presented in Table 2.

Centrum length increases steadily from the third vertebra to the region of vertebra 14, and then remains relatively constant throughout the dorsal series, ranging between 36 mm (centrum 16) and 46 mm (centrum 35) in length. In the posterior dorsal region, vertebrae 46-48 are somewhat disarticulated and appear to be deformed and heavily pitted on both their lateral surfaces and articular facets. It is unclear whether this is due to post-depositional processes, or if these vertebrae are pathological. Centrum length gradually reduces in the anterior caudal series from 40 mm (centrum 47) to 27 mm (centrum 76); however, it is not possible to consistently quantify centrum height in this same series. The preserved portion of the axial column ends at vertebra 90, which is interpreted to be just anterior to, or in, the apical series, as there is a marked decrease in centrum height in this region.

The neural arches increase gradually in height beginning with the first visible neural arches at approximately vertebra 7, up to a maximum height near vertebra 29 in the anterior to mid dorsal region, where they are also longest anteroposteriorly. The degree to which the neural spines are inclined posteriorly also increases in the mid dorsal region compared to the more anterior vertebrae, which are more vertically inclined. All of the preserved presacral neural arches have a V-shaped apical notch in the neural spines as seen in lateral view, with the anterior and posterior margins being higher than the midpoint of the apex (Figure 7). In dorsal view, the spine also bears a depression or concavity at its apex. This notched condition was not observed in any of the caudal series. The posteriormost dorsal and anterior caudal neural arches are not visible, but neural arches in the middle of the preflexural series are very short, anteroposteriorly compressed and nearly rod-like and steeply inclined posteriorly. Because the neural arches remain largely in articulation, the morphology and orientation of the zygapophyses are not visible.

The dorsal ribs are all double-headed in the presacral series, are figure-8 shaped in cross section and taper gradually to their distal ends. Rib number 30 is the longest measured rib, which is 92 cm in length, or 0.42 presacral length (Bucholtz, 2001). A few small ribs are preserved on the anterior caudals, but no obvious chevrons can be discerned in the tail region.

Numerous gastralia are preserved with PMO 214.578. The gastralia, all of which have been displaced and disarticulated, are recognisable in being much thinner than dorsal ribs, having a longitudinal groove along one surface throughout their length, and taper to a thin point.

Appendicular skeleton

Pectoral girdle

The morphology of the pectoral girdle is best understood from the left side, which includes a complete and articulated scapula and coracoid, and a nearly complete and partially articulated clavicle and interclavicle (Figure 8).

The scapula comprises an anteroposteriorly expanded proximal blade and a relatively narrower, strap-like distal

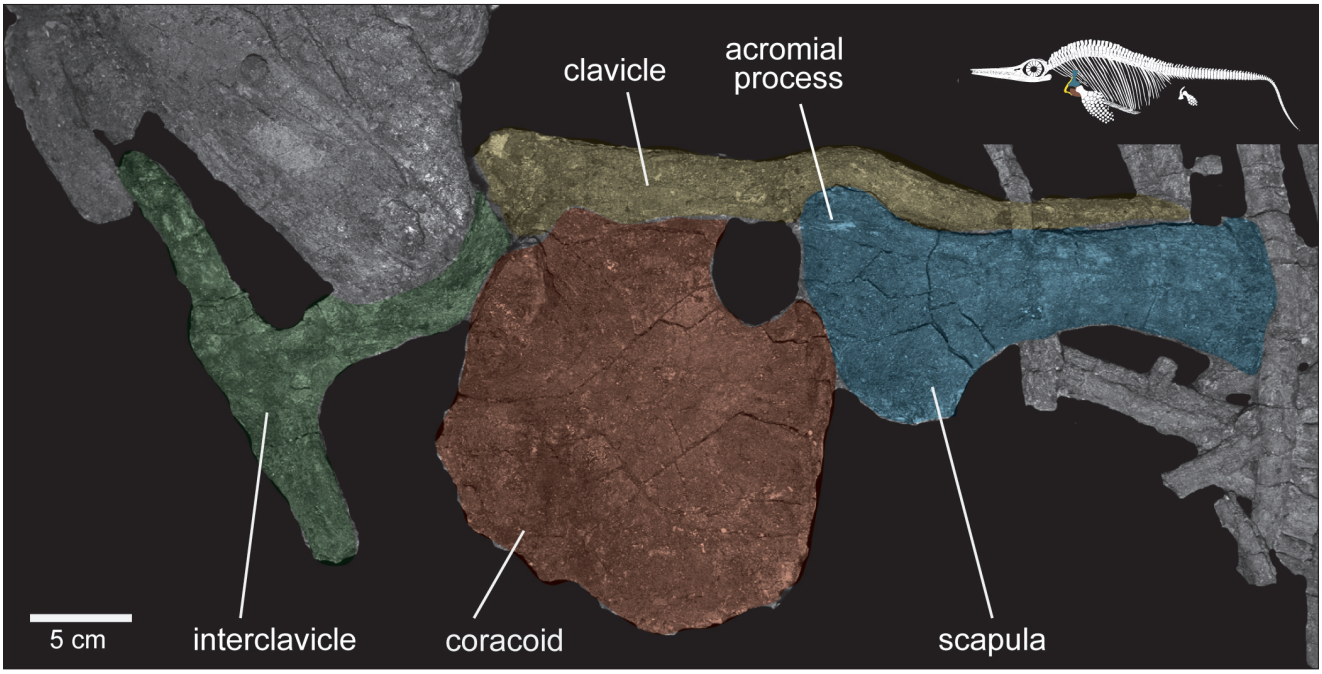

Figure 8. Left pectoral girdle of the holotype specimen of Cryopterygius kristiansenae*, PMO 214.578, as preserved in left-lateral view of the skeleton.*

blade. The articular surface of the proximal end of the scapula can be divided into three major portions; an anterior, non-articular surface that supports the acromial process, as well as the coracoid and glenoid facets. The proximal end of the anterior portion is relatively thin compared to the coracoid and glenoid facets and is medially convex. The anterior portion of the scapula also forms the lateral margin of a prominent coracoid notch but does not bear a facet for a bone to bone contact with the coracoid. The coracoid facet is slightly shorter than the glenoid facet (Table 3). Both facets are relatively thicker than the anterior surface, bear a coarsely pitted surface, and their articular faces converge at an angle of approximately 140 degrees. The proximolateral surface of the scapula bears a broad, shallow concavity, the anterior margin of which is demarked by a well-defined acromial ridge that flares laterally. The distal blade forms approximately two-thirds of the total scapular length, has a nearly straight anterior margin, and a gently concave posterior margin. The anteroposteriorly narrowest point of the scapula lies at its approximate midpoint. The distal end is modestly expanded anteroposteriorly and only slightly thickened mediolaterally compared to the rest of the blade.

The coracoid is anteroposteriorly longer than wide (Table 3). The intercoracoid facet forms the anterior half of the medial margin. Based on the disarticulated right coracoid, this facet is mediolaterally thickened and bears a coarsely textured surface for articulation with the right element via a soft tissue (cartilaginous?) connection. The anterior process is prominent and forms the medial border of an anterolaterally directed coracoid notch. The scapular facet is relatively small, being approximately half the length of the glenoid facet (Table 3). The long axis of the glenoid facet lies in the parasagittal plane and thus faces laterally rather than posterolaterally. The posterior border of the coracoid is broadly convex and has a crenulated margin, suggesting investment in soft tissue.
Much of the left clavicle is preserved. Its proximal half lies external to the coracoid and overlaps its anteriormost margin; whether this position is a taphonomic artifact or represents its actual position in life is equivocal. The distal portion of the clavicle lies largely anterior to the laterally directed flange of the acromial process of the scapula, and then ascends the anterior margin of the scapular blade before terminating approximately 25 mm from its distal end.

A complete interclavicle is preserved and is largely complete but is displaced from the rest of the pectoral girdle. The lateral rami are shallowly depressed on their dorsal surfaces and gradually taper in anteroposterior length distally. The posterior ramus expands markedly in mediolateral width posteriorly, forming a broad spatulate process that is widest slightly posterior to its midpoint.

Forefin

PMO 214.578 possesses a nearly complete forefin that remains in articulation with the pectoral girdle (Figures 2, 9). Both taphonomic and morphologic evidence support the limb's identity as being a left forefin. PMO 214.578 was found lying on its left side in a largely articulated state, with the forelimb still articulated into the well preserved and articulated glenoid fossa of the left pectoral girdle. The articulated humerus of PMO 214.578

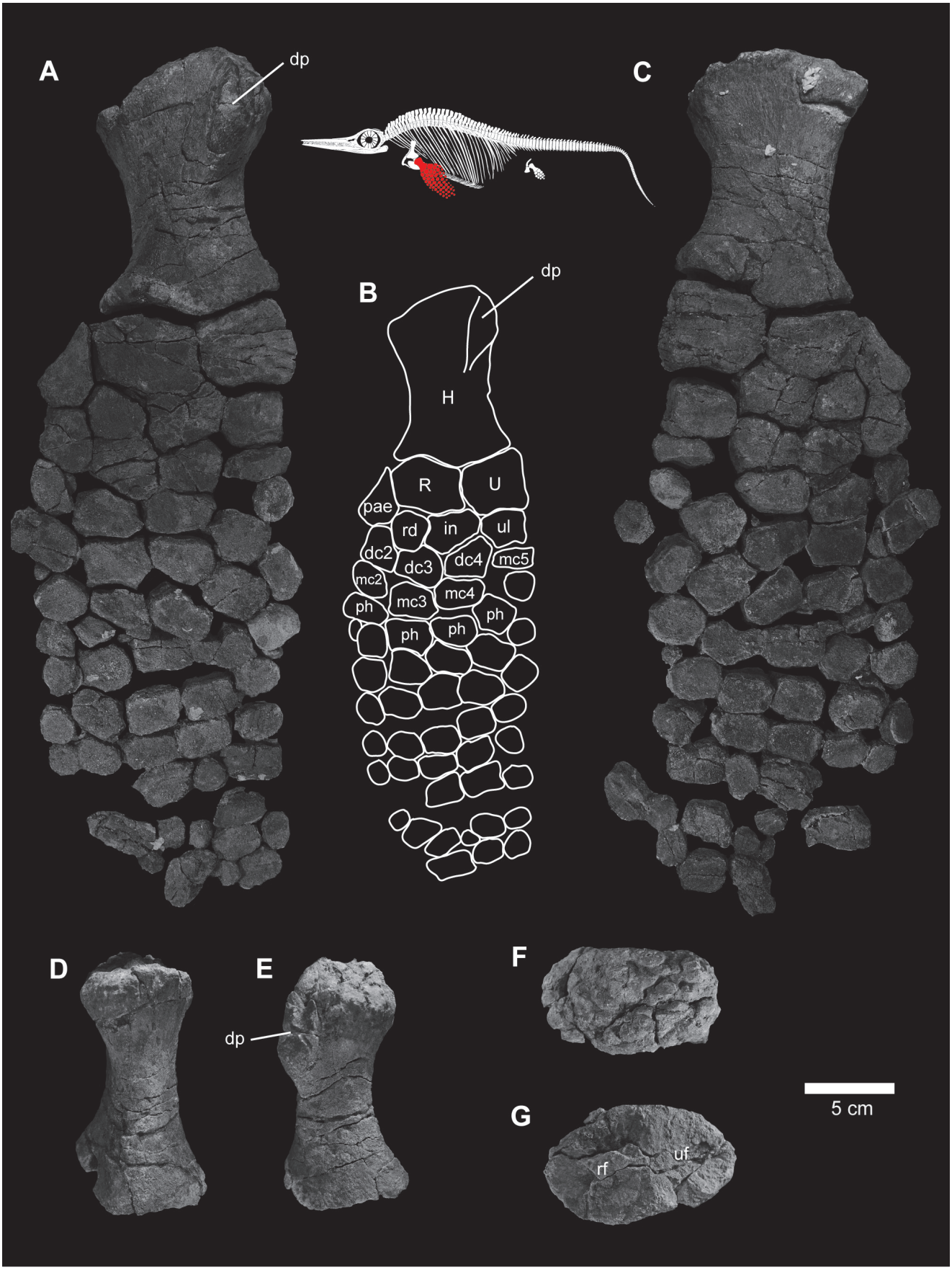

Figure 9. Left forelimb of the holotype specimen of Cryopterygius kristiansenae, *PMO 214.578. Photo (A) and interpretation (B) in dorsal views and photo in ventral (C) view. Left humerus in anterior (D), posterior (E), proximal (F) and distal (G) views. Abbreviations: dc, distal carpal; dp, dorsal process; H, humerus; in, intermedium; mc, metacarpal; pae, preaxial accessory element; ph, phalanx; R, radius; rd, radiale; rf, radial facet; U, ulna; uf, ulnar facet; ul, ulnare.*

Table 3: Selected pectoral girdle measurements of PMO 214.578 (in mm).	
Coracoid	
Maximum mediolateral width	185
Maximum anteroposterior length	225
Length of intercoracoid suture	145*
Length of scapular facet	40
Length of glenoid facet	95
Scapula	
Maximum proximodistal length	240
Maximum anteroposterior width, proximal blade	125
Minimum anteroposterior width, middle of blade	50
Maximum anteroposterior width, distal blade	75
Length of the coracoid facet	40*
Length of the glenoid facet	60*
Interclavicle	
Maximum mediolateral width	220
Maximum length of medial ramus	180

* estimated dimension

Table 4: Selected forelimb measurements of PMO 214.578 (in mm).	
Humerus	
Maximum proximodistal length	155
Maximum anteroposterior width, proximal end	115
Maximum height, proximal end	65
Maximum anteroposterior width, distal end	111
Maximum height, proximal end	57
Mimimun anteroposterior width, midshaft	73
Length of radial facet	59
Length of ulnar facet	59
Radius	
Maximum proximodistal length	45
Maximum anteroposterior width	63
Dorsoventral thickness, proximal end	50
Ulna	
Maximum proximodistal length	55
Maximum anteroposterior width	62
Dorsoventral thickness, proximal end	45

was also compared to left humeri of *Ophthalmosaurus* (NHMUK R.2134 and others) that were oriented following the work of Kirton (1983). As summarised in McGowan & Motani (2003), the dorsal process is more prominent than the deltopectoral crest. The dorsal process arises from the postaxial margin and its long axis trends anteriorly and distally toward the midline. The preaxial margin of the humerus is relatively thinner and sharper than the more broadly rounded postaxial margin. These features used to recognise the left humerus of *Ophthalmosaurus* were wholly consistent with those found in the articulated left humerus of PMO 214.578.

In its general proportions, the forefin appears relatively small in both length and width compared to overall body length (55 cm long as preserved; estimated 65-70 cm total length), although some of the distalmost phalanges are missing. In dorsal aspect, the paddle is asymmetrical in outline with respect to its long axis, being more broadly expanded preaxially than postaxially. The preaxial margin is gently rounded and convex anteriorly; the postaxial margin appears relatively straight, but some of the elements have been displaced in this region.

Humerus

The proximal and distal ends of the humerus are nearly identical in maximum anteroposterior width (Table 4). The proximal articular surface is anteroposteriorly longer than dorsoventrally tall (Table 4; Figure 9) and is very irregular and bears prominent "hummocks" and intervening "swales", suggesting a considerable investment in articular cartilage. A prominent dorsal process is situated entirely on the posterior half of the humerus. It arises near the posterodorsal surface, extends distally and anteriorly, and ends abruptly by the midpoint of the shaft. In dorsal view, the shaft is moderately constricted giving the humerus a length to midshaft width ratio of 2.12. Ventrally, the deltopectoral crest is very weakly developed and is only represented by a low ridge that is situated in the posterior half of the humerus. Distally, the humerus bears two large articular facets for the radius and ulna that are equal in anteroposterior length. Significantly, a facet for a preaxial accessory element is absent on the left humerus (although a very diminutive "facet" is present on the right humerus). In dorsal view, the radial and ulnar facets of the humerus meet at an angle of approximately 30 degrees.

Zeugopodium and autopodium

The identity of digits is based on the criteria developed for recognising the primary axis of the forelimb by Motani (1999). The radius and ulna are recognised as the two largest anterior and posterior elements, respectively. Both elements are polygonal and slightly broader than long, with the radius being slightly larger than the ulna (Table 4). The ulna articulates with the ulnare distally, and has a short contact with the intermedium along its anterodistal margin. The distal margin of the radius is shared approximately equally with the intermedium and radiale. A preaxial accessory element contacts much

of the anterior margin of the radius but does not contact the humerus (although a very small preaxial facet is present on the right humerus). In dorsal view the preaxial accessory element is roughly teardrop-shaped in outline, being anteroposteriorly broadest distally, but dorsoventrally thickest proximally. In cross-sectional profile, it is wedge-shaped and is dorsoventrally thinnest along its preaxial margin. It bears distinct facets for the radiale and distal carpal 2.

Preaxially to postaxially, the identity of the radiale, intermedium and ulnare are easily established based on their topology relative to the epipodial row (Figure 9). All three elements are polygonal and broader than long, with the intermedium being broadest both relatively and in absolute dimensions. The homology of the more distal limb elements, including the correct identification of digit number is more ambiguous and two alternatives are presented. The preferred interpretation (Figure 9) recognises distal carpal 4 to lie distal and slightly anterior to the ulnare and form much of the distal margin of the intermedium (Motani, 1999). Thus, distal carpal 4 defines the base of digit IV and the identity of other digits. Distal carpal 2 and 3 form the distal margins of the preaxial accessory element and radiale, respectively. Metacarpal 5 lies distal to the ulnare and posterior to distal carpal 4. The ulnare lacks a facet along its postaxial margin, suggesting a primary absence of a pisiform. The distal portion of the forelimb is comprised of five definitive digits, identified (preaxially to postaxially) as digits II, III, IV, V, and a single postaxial accessory digit. In this preferred interpretation, the presence of a preaxial accessory digit – a diagnostic feature of Ophthalmosauridae – appears to be absent. However, the presence of a second anteriorly positioned facet at the distal end of the preaxial accessory element, as well as along the anterior margin of distal carpal 2, suggests that the preaxial accessory digit may have been present but was poorly preserved or lost during collection.

A second interpretation recognises the anteriormost complete digit as the preaxial accessory digit. However, this interpretation results in an alternative and less satisfactory relationship between the proximal and distal carpal rows. In this scenario, distal carpal 4 would occupy the posteriormost position in the distal carpal row, resulting in the loss of metacarpal V, which typically contacts the ulnare. Additionally, distal carpal 4 would no longer contact the intermedium, as it does in most other ophthalmosaurids (Motani, 1999).

The phalanges vary considerably in shape. The proximal phalanges are polygonal, whilst those of digit IV and V from the middle of the limb are subrectangular and broader than long. The distalmost preserved phalanges, as well as those found along the pre- and postaxial margins are subrounded.

Pelvic girdle and hindfin

PMO 214.578 is exceptional in preserving one complete side of the pelvic girdle and much of a hindfin in articulation (Figure 10). Based on taphonomic evidence, the left pelvic girdle and limb are preserved. Similar to the pectoral girdle and dorsal ribs, the left side of the pelvic girdle was in direct contact with the sediment and appears to have been protected from significant disturbance as the carcass lay on the sea-floor. The medial surface of the left ilium came to rest in direct contact with the vertebral column, while the ischiopubis lies ventral to it. The femur remains articulated into the acetabulum and appears to have folded dorsally in the transverse plane over the vertebral column, so that its dorsal surface is now in direct contact with the left surface of the articulated anterior caudal vertebrae. In this regard, the hindfin is preserved in a manner nearly identical to that of the referred specimen of *Caypullisaurus bonapartei*, MLP 83-XI-16-1 (Fernández, 2007). This location permitted the tibia, fibula and two proximal epipodials to remain in articulation, but all portions of the fin distal to this point (extending beyond the vertebral column) are lost.

Pelvic girdle

As preserved, the left ilium lies with its medial surface in contact with vertebra number 53 and 54. The shaft of the ilium is not rod-like; rather, it is mediolaterally flattened and is anteroposteriorly broadest in its proximal half (Figure 10). The long axis of the ilium is gently sigmoid in shape. The proximal end is gently convex and at its distal end, two distinct facets are visible; a small anterior facet for the ischiopubis, and a larger, posteroventrally facing acetabular facet. The ischium and pubis are fused proximally for approximately two-thirds of their length but are split distally by a prominent notch, presumably

Table 5: Selected pelvic girdle measurements of PMO 214.578 (in mm).

Ilium	
Maximum proximodistal length	130
Maximum anteroposterior width, proximal half	35
Maximum height (thickness), proximal end	35
Maximum anteroposterior width, distal end	45
Length of ischiopubis facet	7*
Length of acetabular facet	27*
Ischiopubis	
Maximum proximodistal length	175
Maximum anteroposterior width, proximal end	48*
Dorsoventral thickness, proximal end	10*
Maximum anteroposterior width, distal end	110
Length of the ischiopubic notch	45*

* estimated dimension

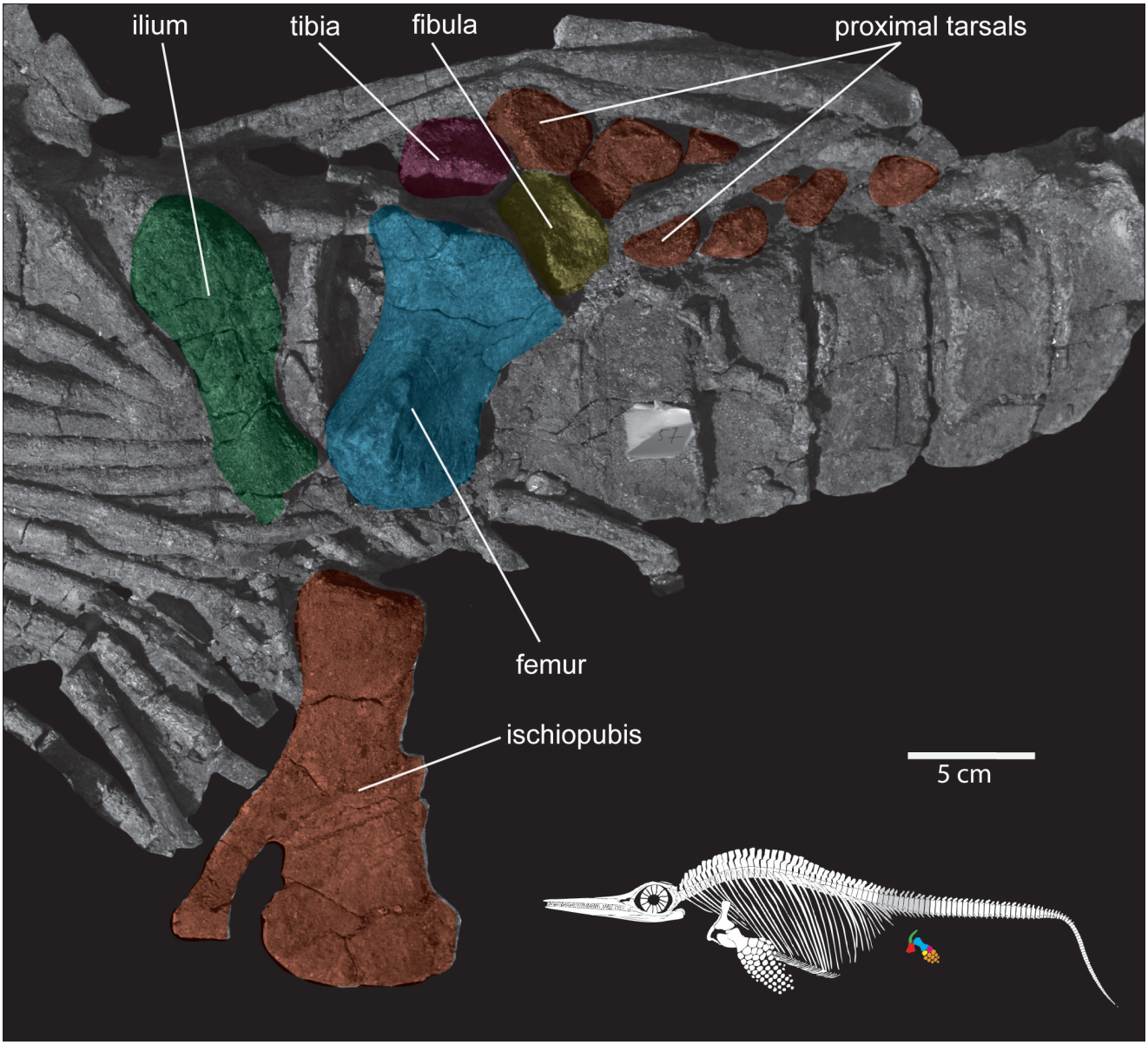

Figure 10. Left pelvic girdle and hind limb of holotype specimen of Cryopterygius kristiansenae, *PMO 214.578 in left-lateral view. The articulated femur is folded dorsally over the vertebral column, exposing its ventral surface in this view.*

homologous to an open ischiopubic (or obturator) foramen. The notch is located closer to the anterior margin than the posterior margin. The proximal end of the ischiopubis is mediolaterally thicker than the distal plate-like end and bears a single well defined facet, although the articular surface is not completely exposed. The distal half of the ischiopubis expands to approximately 2.3 times the anteroposterior width of the anterior end (Table 5), with the ischium being markedly wider than the pubis. At its distal end, the ischiopubis appears uniformly thin.

Femur and zeugopodium

The preservation of an articulated femur in PMO 214.578 facilitates the first accurate orientation of an ophthalmosaurid femur (Maxwell *et al.*, 2012). The proximal articular surface of the femur is undulating and irregular, but is not as conspicuously hummocky as that seen on the humerus. The proximal end is narrower in maximum anteroposterior width than the distal end (Table 6; Figure 11). In proximal articular view, the femur is dorsoventrally taller than wide. The dorsal surface is relatively flatter than the ventral surface and bears a low, broadly rounded dorsal process that is situated close to the anterior margin of the femur (Figure 11). A prominent and well-defined ventral process extends slightly less than half the proximodistal length of the femur. The process is located nearly equidistant from the anterior and posterior margins of the femur. In either proximal or distal view, the entire ventral process tilts slightly anteriorly and its anterior surface is somewhat more concave than the posterior surface. The anterior surface of the femur

is a dorsoventrally tall, relatively flat face that is bounded dorsally by the low, dorsal process and ventrally by the ventral process. In proximal articular view, the anterior margin is slightly convex (Figure 11). The posterior margin of the femur tapers posteriorly to a thin blade-like margin that is concave in outline in dorsal view. At its midpoint, the femoral shaft constricts only slightly in anteroposterior width compared to the proximal end, but the distal end is expanded, particularly along its anterior margin. The distal end of the femur bears only two articular facets; both the tibial and the fibular facets are equal in anteroposteriorly width (Table 6). In outline, the tibial facet is more narrowly triangular in distal view compared to the more oval fibular facet. In dorsal view, the plane of the tibial facet lies nearly at right-angles to the long axis of the femur and faces almost directly laterally. In contrast, the fibular facet faces posterolaterally at an angle of approximately 45 degrees to the long axis of the femur.

The distal portion of the hindfin is incomplete, but includes a partially articulated tibia and fibula, and astragalus and calcaneum. The tibia and fibula are polygonal in shape with the former slightly smaller than the latter. The astragalus contacts both the tibia and the fibula and is somewhat more rounded in outline. The shape of the calcaneum is hard to discern as preserved. Based on the articular facets of the preserved portion of the limb, at least three digits were present in the hindfin.

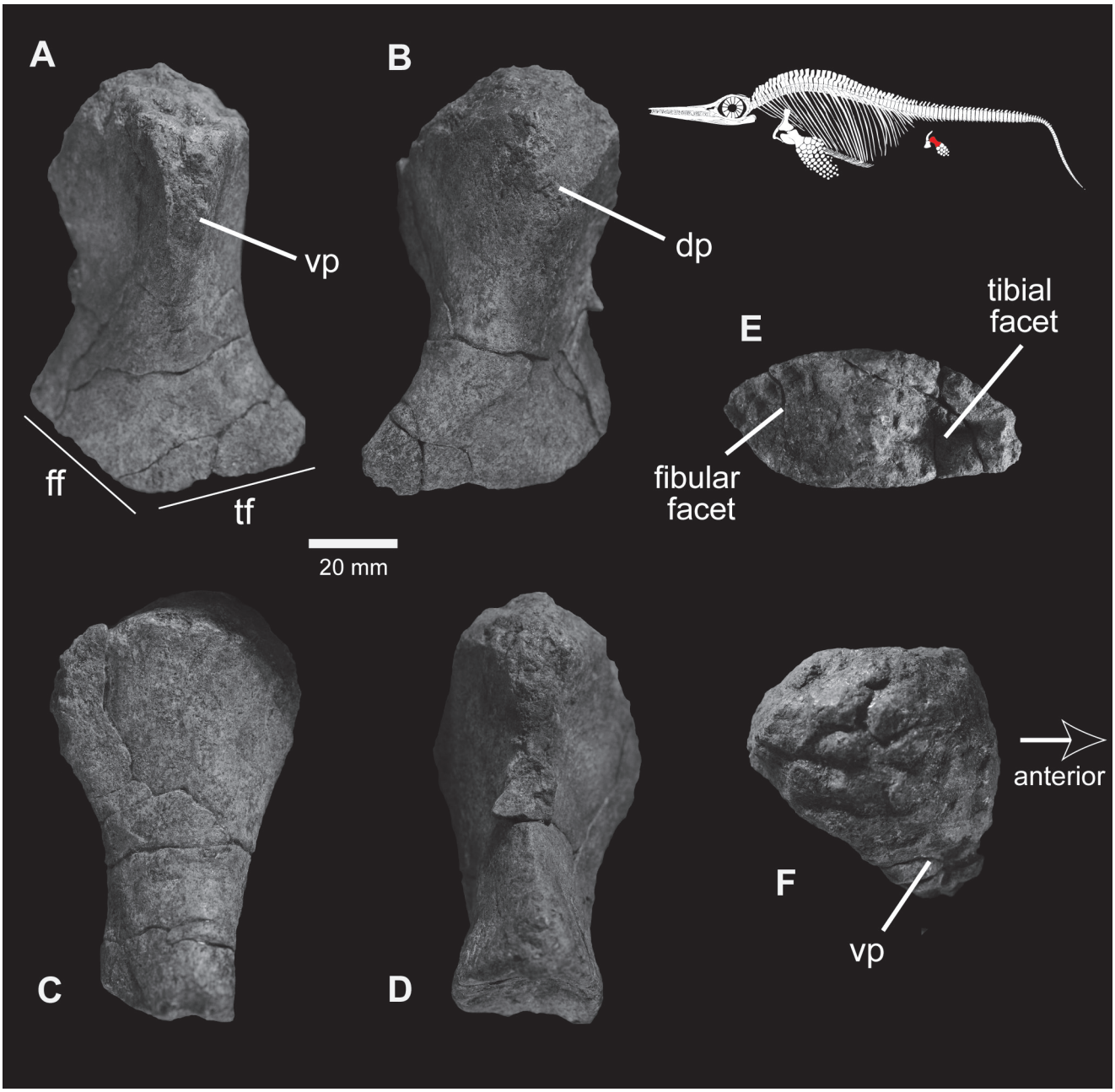

Figure 11. Left femur of the holotype specimen of Cryopterygius kristiansenae, *PMO 214.578 in ventral (A), dorsal (B), anterior (C), posterior (D), distal (E) and proximal (F) views. Abbreviations: dp, dorsal process; ff, fibular facet; tf, tibial facet; vp, ventral process.*

Table 6: Selected hindlimb measurements of PMO 214.578 (in mm).	
Femur	
Maximum proximodistal length	112
Maximum anteroposterior width, proximal end	58
Maximum height, proximal end	68
Maximum anteroposterior width, distal end	83
Maximum height, proximal end	34
Mimimum anteroposterior width, midshaft	50
Length of tibial facet	45
Length of fibular facet	45
Tibia	
Maximum proximodistal length	30*
Maximum anteroposterior width	40
Dorsoventral thickness, proximal end	20*
Fibula	
Maximum proximodistal length	30
Maximum anteroposterior width	45
Dorsoventral thickness, proximal end	30*

* estimated dimension

Systematic Paleontology

ICHTHYOSAURIA de Blainville, 1835
OPHTHALMOSAURIDAE Baur, 1887

Palvennia gen. nov.

urn:lsid:zoobank.org:act:98D18CE4-1C3A-494C-BE94-F884B263D5D3
Type and only species – *Palvennia hoybergeti* sp. nov
Type locality – north side of Janusfjellet, approximately 13 km northeast of Longyearbyen, Spitsbergen, Norway. UTM WGS84 33N 0518775 8696150
Type horizon and stage – Slottsmøya Member, Agardhfjellet Formation, Middle Volgian, Upper Jurassic; 15.2 metres below the *Dorsoplanites* bed within the *Dorsoplanites ilovaiskyi* to *D. maximus* zones (Nagy & Basov, 1998; Collingnon & Hammer, 2012; Gradstein *et al.*, 2012).
Etymology – *Palvennia* from PalVenn (Friends of the Palaeontological Museum in Oslo), whose anniversary expedition in 2004 led to the discovery of SVB 1451.
Diagnosis – as for species

Palvennia hoybergeti sp. nov.
(Figures 12-21)
urn:lsid:zoobank.org:act:03BA5E23-17B5-4AB1-B98A-681B9968A3F9

Holotype – SVB 1451, a nearly complete skull, atlas/axis complex, proximal and distal portions of a humerus and isolated distal limb elements and several disarticulated dorsal ribs.

Etymology – *hoybergeti*, in honour of Magne Høyberget of Mandal, Norway, long-time participant in the Spitsbergen Jurassic Research Group fieldwork on Spitsbergen.

Differential diagnosis – moderately large ophthalmosaurid ichthyosaur (skull length 86 cm) with the following autapomorphies and unique character combinations: relatively short rostrum with snout ratio of 0.59 (relatively longer in *Caypullisaurus* and more gracile in *Aegirosaurus*, *Nannopterygius*); very large orbit (comparatively smaller in *Cryopterygius*, *Brachypterygius*, *Caypullisaurus*); strongly bowed jugal (relatively straight in *Cryopterygius*, *Brachypterygius*); narrow postorbital bar (broad in *Cryopterygius*, *Caypullisaurus*); frontals mediolateral broad on skull roof (little frontal exposure on skull roof in *Athabascasaurus*, *Ophthalmosaurus*); long frontal-postfrontal contact (short in *Platypterygius australis*, *Ophthalmosaurus*); very large pineal foramen (autapomorphic); extracondylar area of basioccipital not visible in posterior view (visible in *Ophthalmosaurus*, *Sveltonectes*, *Acamptonectes*) and lacking a ventral notch (ventral notch in *Ophthalmosaurus*, *Mollesaurus*); lateral and ventral surface of basioccipital with broad extracondylar area of finished bone (very narrow extracondylar area in *Sveltonectes*, *Brachypterygius*); anterior face of basioccipital lacks notochordal pit and basioccipital peg (both present in *Arthropterygius*); ventral facet of exoccipital not anteriorly elongate (elongated in *Brachypterygius*, *Ophthalmosaurus*, *P. australis*, *Acamptonectes*); gracile and constricted stapedial shaft (robust shaft without constriction in *P. australis* and *Ophthalmosaurus*); facet for preaxial accessory element (absent in *Cryopterygius*, *Nannopterygius*, *Sveltonectes*).

Description

General comments

SVB 1451 consists primarily of a nearly complete skull that is obliquely dorsoventrally compressed (Figures 12-15). The specimen was collected out of permafrost and has been extensively fractured due to congelifraction. Both surfaces of the skull block have been prepared; one side presents the dorsal and partial left-lateral surface while the reverse side presents most of the lower jaws, the posterior portion of the palate, and the poorly preserved right cheek area. Elements of the dermatocranium remain largely articulated and their relationships can be largely discerned; however, the cheek regions on both the right and left sides are damaged and most of the braincase has become disarticulated and displaced posteriorly. The postcranial elements are fragmentary and disarticulated.

Ontogeny

Many of the typical ontogenetic indicators, especially most of those relating to the limbs (Johnson, 1977), are not available for this specimen, although the small

Table 7: Selected cranial dimensions of SVB 1451 (in mm).	
Approximate skull length (premaxilla to posterior margin of postorbital bar)	860
Preorbital length	540
Length of orbit as preserved	290
Length of premaxilla along toothrow	390
Length of maxilla	210
Anteroposterior length of postorbital bar	33
Maximum length of lower jaw	910
Maximum length of pineal foramen	73
Maximum width of pineal foramen	45
Maximum length of supratemporal fenestra (left)	130
Combined width of parietals at midpoint of supratemporal fenestra	110
Maximum mediolateral width of anterior surface of basioccipital	72
Maximum height of posterior surface of basioccipital	54
Anteroposterior length of basioccipital along ventral margin	41
Anteroposterior length of basioccipital along dorsal margin	59

amount of surface bone on the humeral fragment is smooth and does not suggest immaturity. There is no indication that cervical centrum 3 was fused to the atlas-axis complex (a possible ontogenetic indicator; Maxwell & Kear, 2010), but the complex itself is well fused. However, the skull is relatively large (86 cm in length; Table 7) and the limb elements robust. Given the relatively large size and absence of any features clearly suggesting otherwise, SVB 1451 is tentatively interpreted to be an adult.

Skull

The rostrum is mediolaterally narrow and pointed anteriorly and has a "snout" ratio of 0.59 (Figures 12, 13). The left premaxilla bears an estimated 27 teeth but is otherwise poorly preserved. The supranarial process is missing and most of the other bones in the region of the external naris are damaged, making it impossible to determine the relationships of the bones in this area.

The orbit is dorsoventrally crushed, influencing its actual anteroposterior dimension (29 cm; Table 7). However, the jugal is 28 cm long, suggesting that the orbital dimensions are not greatly altered. As preserved, the orbit is very large, representing 34 percent of total skull length and having an orbital ratio of 0.32 (although these figures may be somewhat high). Portions of an imperfectly preserved scleral ring are preserved in the left orbit (Figure 16). A small rib-like element was also preserved in the left orbit, but its identity is unclear (Figure 16).

The maxilla is well exposed in lateral profile and forms approximately 36 percent of the total toothrow length and has a maxillary ratio of 0.23. The left maxilla bears approximately 15 teeth. The presence or morphology of a dorsal ascending process cannot be discerned. The posterior end of the maxilla terminates at approximately in line with the anterior one-quarter of the orbital length.

The lacrimal is a robust element and is largely complete. Because it has been somewhat displaced its morphology is readily discerned. The anteroventral portion of the lacrimal bears a prominent anteriorly projecting process; although the subnarial process of the premaxilla is damaged, it seems likely that it contacted and overlapped this lacrimal in this area. It is unclear whether the lacrimal formed the posterior margin of the external naris. The posterior margin of the lacrimal tapers posteriorly to a narrow projection along the ventral margin of the orbit. The position of the displaced jugal suggests that it overlapped at least the posteriormost end of the lacrimal. A prominent yet narrow, gently curving ridge trends anterodorsally to posteroventrally across the lateral surface of the lacrimal.

The jugal is displaced and has rotated 180 degrees about its long axis (Figures 12, 13). It is conspicuously bowed but other details about its relationships to the lacrimal and postorbital bones cannot be discerned. The postorbital bar is largely complete and is dorsoventrally tall and conspicuously narrow mediolaterally (Table 7); however, the contacts between the postorbital and quadratojugal are not visible, and contacts with other elements cannot be confidently discerned.

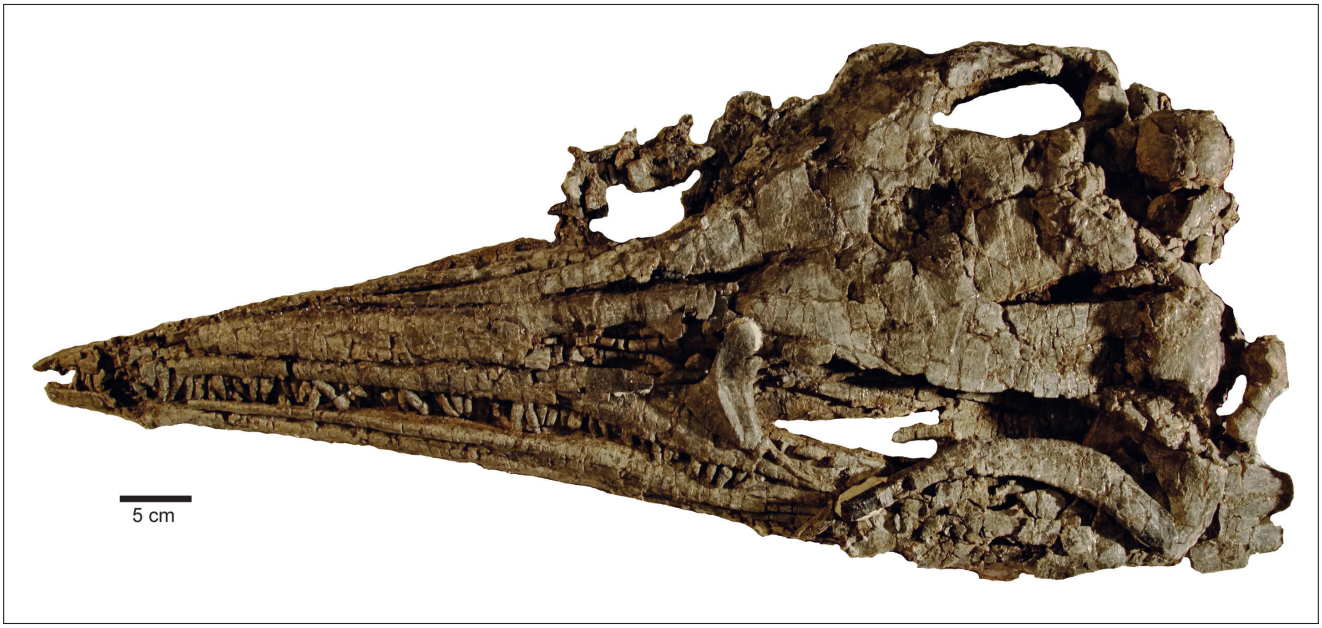

Figure 12. Photograph of the holotype skull of Palvennia hoybergeti, *SVB 1451, in oblique left-dorsal view.*

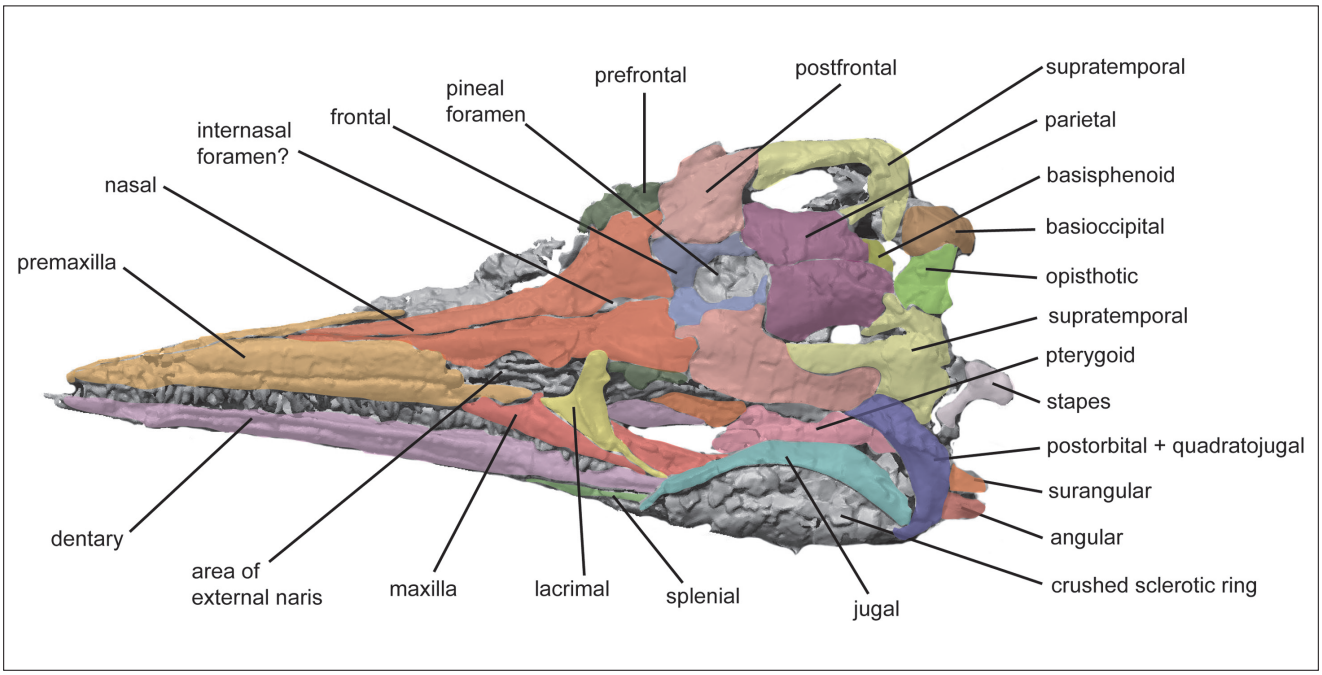

Figure 13. Interpretation of the holotype skull of Palvennia hoybergeti, *SVB 1451, in oblique left-dorsal view.*

Although fragmented and slightly displaced, the relationships of the bones on the dorsal surface can be easily discerned (Figures 12, 13). The nasals are first visible anteriorly on the dorsal surface of the skull approximately 17 cm from the tip of the rostrum. The nasals are loosely sutured along the dorsal midline; an internasal fenestra is difficult to discern, but if present at all, it would be represented by a slight separation of the elements near their posterior ends. The nasals closely approach but do not border the pineal foramen.

The frontals are bordered laterally entirely by the postfrontals, and posterolaterally by the parietals, which it overlaps. The frontals form almost the entire margin of the pineal foramen except at their posterior end, where it is bordered by the parietals. On the left side, the posterior margin of the frontal bears a small projection that extends medially to form almost the entire posterior border of the pineal foramen. The diameter of the pineal foramen is conspicuously large (Table 7), is widest near its midpoint, and is anteroposteriorly longer than

Figure 14. Photograph of the holotype skull of Palvennia hoybergeti, *SVB 1451, in oblique right-ventral view.*

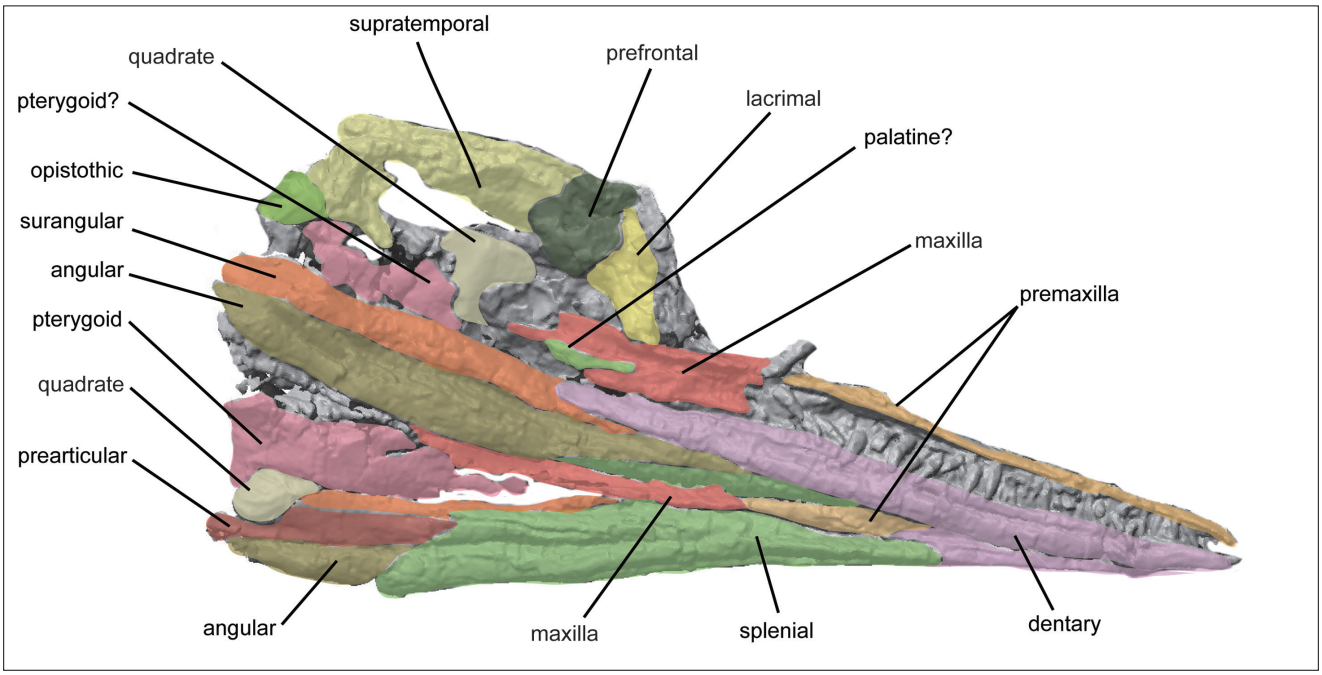

Figure 15. Interpretation of the holotype skull of Palvennia hoybergeti, *SVB 1451, in oblique right-ventral view.*

mediolaterally broad. Elements of the palate (pterygoid?) are visible below the pineal opening.

The left prefrontal extends posteriorly approximately one-third of the orbital length. It likely contacts the lacrimal anteriorly, and shares a short contact with the postfrontal posteriorly.

The postfrontal is a prominent element with well-defined sutures. It underlaps the nasals along its anterior margin, and overlaps the frontals anteromedially. The postfrontal forms the anterolateral margin of the supratemporal fenestra, and closely approaches, but does not contact, the pineal foramen. The postfrontal shares a long contact with the supratemporal and posteriorly it appears to contact the postorbital, but the nature of this contact is not possible to discern due to poor preservation.

The parietals are well preserved and are mediolaterally broad (Table 7) and massive. They form a small portion

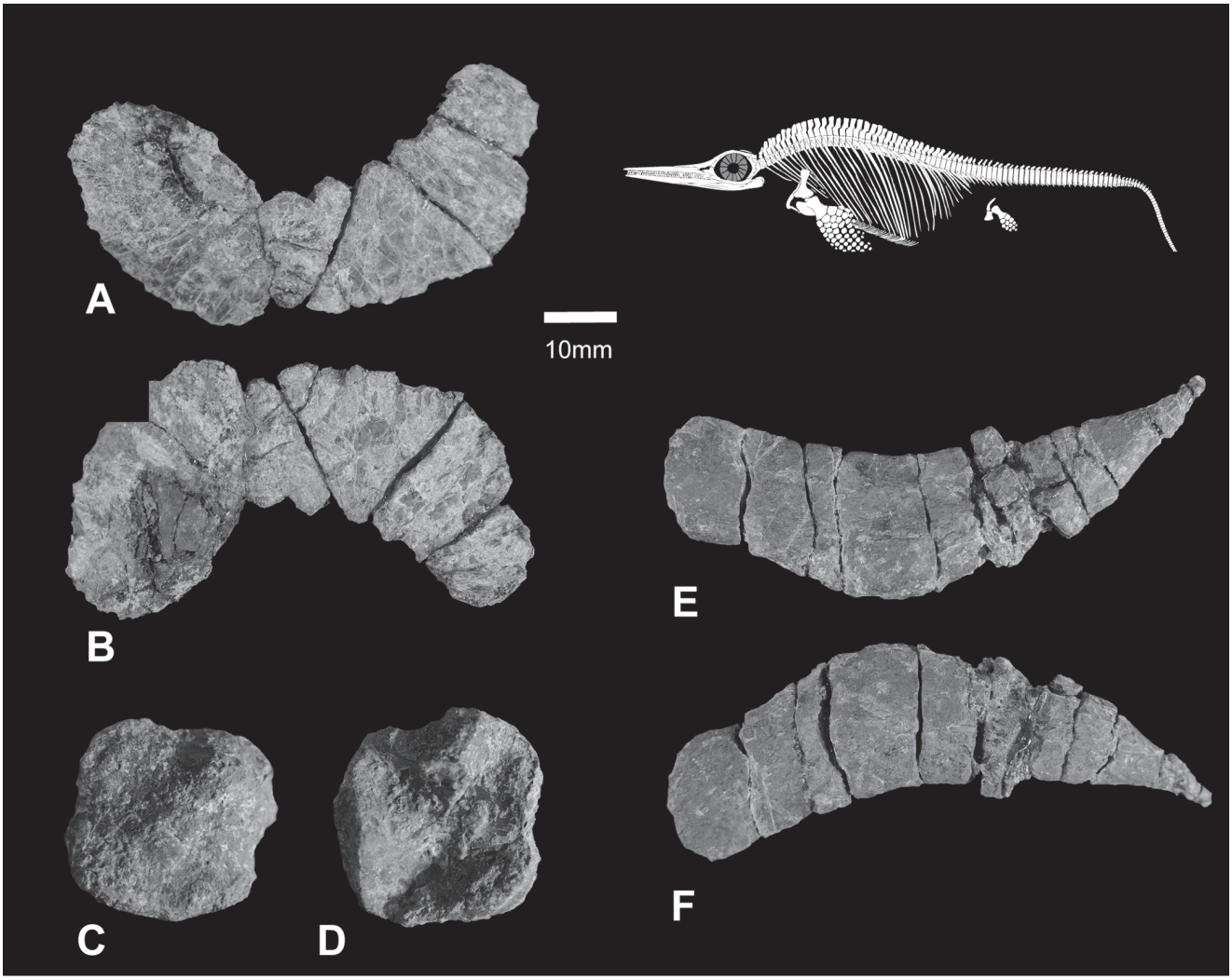

Figure 16. Elements recovered in the orbit of the holotype specimen of Palvennia hoybergeti, *SVB 1451. Partial scleral ring in external (A) and internal (B) views, right(?) prootic in anterior (C) and posterior (D) views, and unidentified element found in the left orbit (E, F).*

of the posterior margin of the pineal foramen. There is no indication of any ornamentation or crest along its dorsal surface. Posteriorly, the parietals form a short posterolateral process that contacts the supratemporals. The supratemporal fenestrae are anteroposteriorly longer than broad although crushing makes it difficult to determine its original shape with confidence.

The supratemporal forms the lateral, posterior and posteromedial margin of the supratemporal fenestra. It also forms most of the posterior margin of the postorbital bar, but its specific relationships to the postorbital and quadratojugal are not clear. The supratemporal forms the posterodorsal margin of the skull, but the presence or absence of a squamosal is equivocal due to poor preservation in this area.

The braincase is represented by the basioccipital, supraoccipital, an exoccipital, both stapes, and a prootic. The basisphenoid, opisthotic and quadrate are also preserved but are largely covered by other elements of the skull or too poorly preserved for description.

The basioccipital (Figure 17) is largely complete and its features well defined, although it is fractured and has some damage along its anterior face. As seen in occipital view, the extracondylar area is not visible, being blocked from view almost entirely by the condylar surface. The occipital condyle is oval in outline, being slightly broader mediolaterally than tall (Table 7). It bears a notochordal pit near its centre, but otherwise lacks pitting or grooves on its condylar surface. In lateral view, the basioccipital is anteroposteriorly broader in its dorsal half. Similarly, the condyle is asymmetrical in profile and appears to be directed slightly ventrally. A broad extracondylar surface of finished, periosteal bone is present along the lateral surfaces, but becomes anteroposteriorly narrower along the ventral margin. A ventral notch is absent. The anterior face of the basioccipital, where it contacts the basisphenoid, is slightly pitted, largely flat, and lacks any indication of a peg or furrow. A notochordal pit is absent on the anterior surface. Dorsally, the surface of the basioccipital is nearly flat and the facets for the exoccipitals are present but poorly preserved.

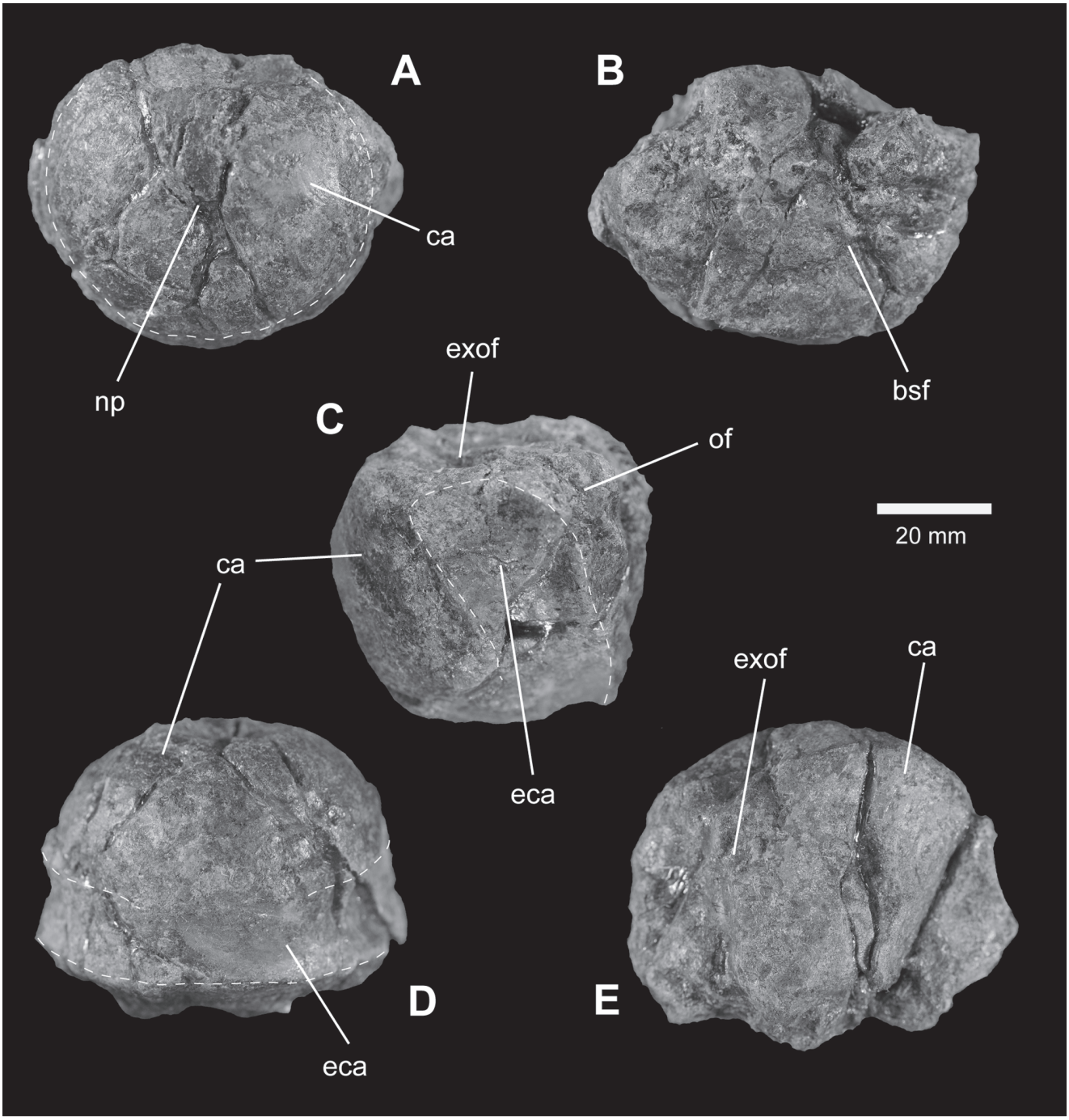

Figure 17. Basioccipital of Palvennia hoybergeti*, holotype specimen of SVB 1451 in posterior (A), anterior (B), right-lateral (C), ventral (D) and dorsal (E) views. Dashed lines in A delimit the margin of the condylar area; dashed lines in C and D delimit the extracondylar area. Abbreviations: bsf, basisphenoid facet; ca, condylar area; eca, extracondylar area; exof, exoccipital facet; np, notochordal pit; of, ophisthotic facet.*

A single left exoccipital is exposed (Figure 18). It is slightly taller dorsoventrally than anteroposteriorly long and is widest ventrally in lateral view, where it forms what is interpreted to be a large facet for the basioccipital. The anteromedial wall is concave, the lateral wall nearly flat. There is no evidence of any foramina for cranial nerves perforating the element.

The supraoccipital (Figure 18) is nearly complete and well preserved. In posterior view, it is mediolaterally broader than tall. Its dorsal margin describes a broadly rounded arc. The mediolaterally width of the foramen magnum is constricted at the supraoccipital-exoccipital suture in occipital view; thus, when in articulation with the exoccipital, the overall shape of the foramen magnum is shaped like the number "8", with the upper and lower parts of the "8" being approximately equal in size. Ventrally, the supraoccipital bears an irregular surface where

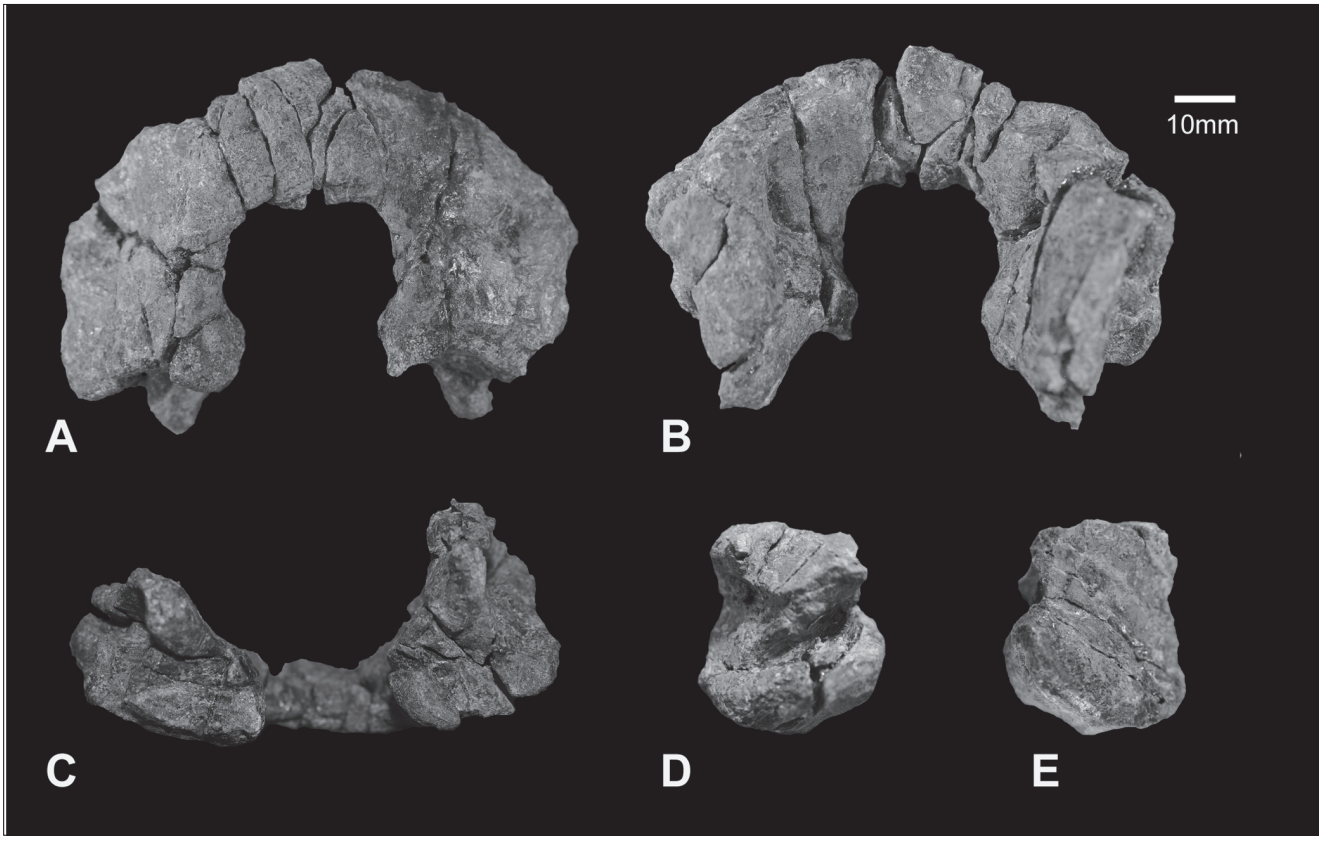

Figure 18. Basicranial elements of SVB 1451, holotype specimen of Palvennia hoybergeti. *Supraoccipital in posterior (A), anterior (B), and ventral (C) views. Left exoccipital in posteromedial (D) and anterolateral (E) views.*

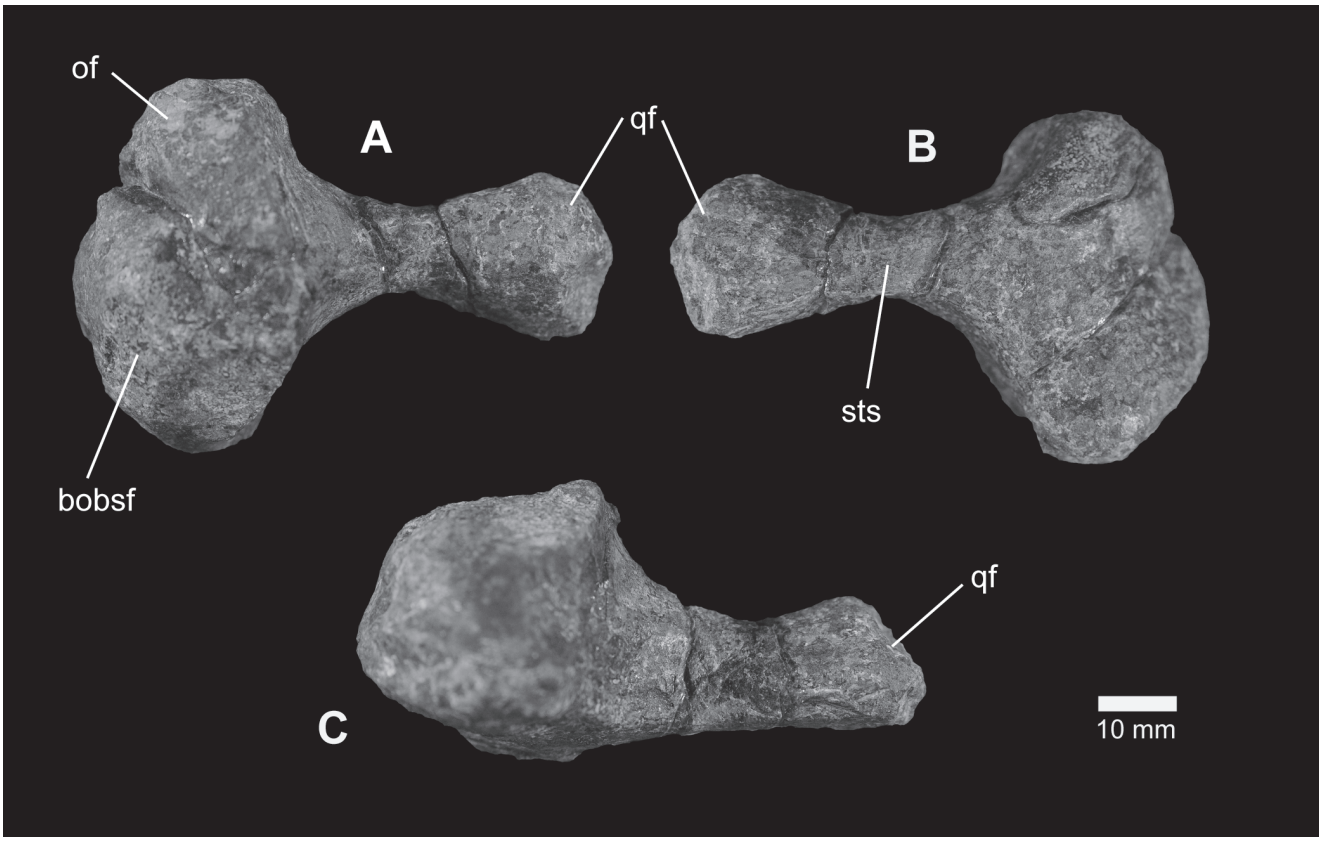

Figure 19. Left stapes of SVB 1451, holotype specimen of Palvennia hoybergeti *in anterior (A), posterior (B) and dorsal (C) views. Abbreviations: bobsf, basioccipital/basisphenoid facet; of, opisthotic facet; qf, quadrate facet; sts, stapedial shaft.*

it contacts the exoccipital, while the ventrolateral margin exhibits a prominent sulcus for the posterior semicircular canal.

The left stapes is complete and has been removed from the skull block (Figure 19). The articular surface of the medial stapedial head is separated by a small horizontally-oriented groove into a smaller, dorsally-situated surface for the opisthotic and larger, ventrally-situated surface for the basioccipital and basisphenoid. The stapedial shaft is very gracile at its midpoint, but expands laterally near the quadrate facet. In dorsal view (Figure 19), the stapedial shaft is situated posteriorly relative to the medial head; its posterior surface nearly straight, while the anterior margin is concave.

The prootic (Figure 16) is complete, somewhat resembles a rounded square in outline, and is equally wide as it is high. The anterior surface is slightly convex while the posterior surface bears well-defined sulci for the anterior and horizontal semicircular canals of the membranous labyrinth.

The palate is poorly preserved, but the posterior ramus of the left pterygoid is exposed on the ventral surface of the skull (Figures 14, 15). The ramus is broadly strap-like and expands mediolaterally posterior to its contact with the quadrate. It is not possible to discern the nature of its contacts with the basicranium or other elements of the palate.

The lower jaws are best interpreted from the ventral side of the skull (Figures 14, 15). As seen on the lateral surface of the right ramus, the dentary terminates approximately in line with the anterior margin of the orbit (posterior margin of the lacrimal). The angular is exposed laterally further anteriorly than the surangular. At their posterior ends, the angular and surangular each contributes approximately equally to the dorsalventral height of the ramus. The splenial is well exposed on the medial surface of the left ramus. It extends anteriorly as far as the midpoint of the rostrum; caudad, its posterior margin slopes posteroventrally and tapers out against, and lying medial to, the angular.

The dentition of *Palvennia* does not conspicuously decrease in crown height along the toothrow anteriorly toward the tip of the rostrum. Maximum crown height is approximately 12 mm, giving a tooth length index of 0.13. Poor preservation limits other details regarding tooth morphology other than that they bear longitudinal enamelled ridges along at least the labial surface.

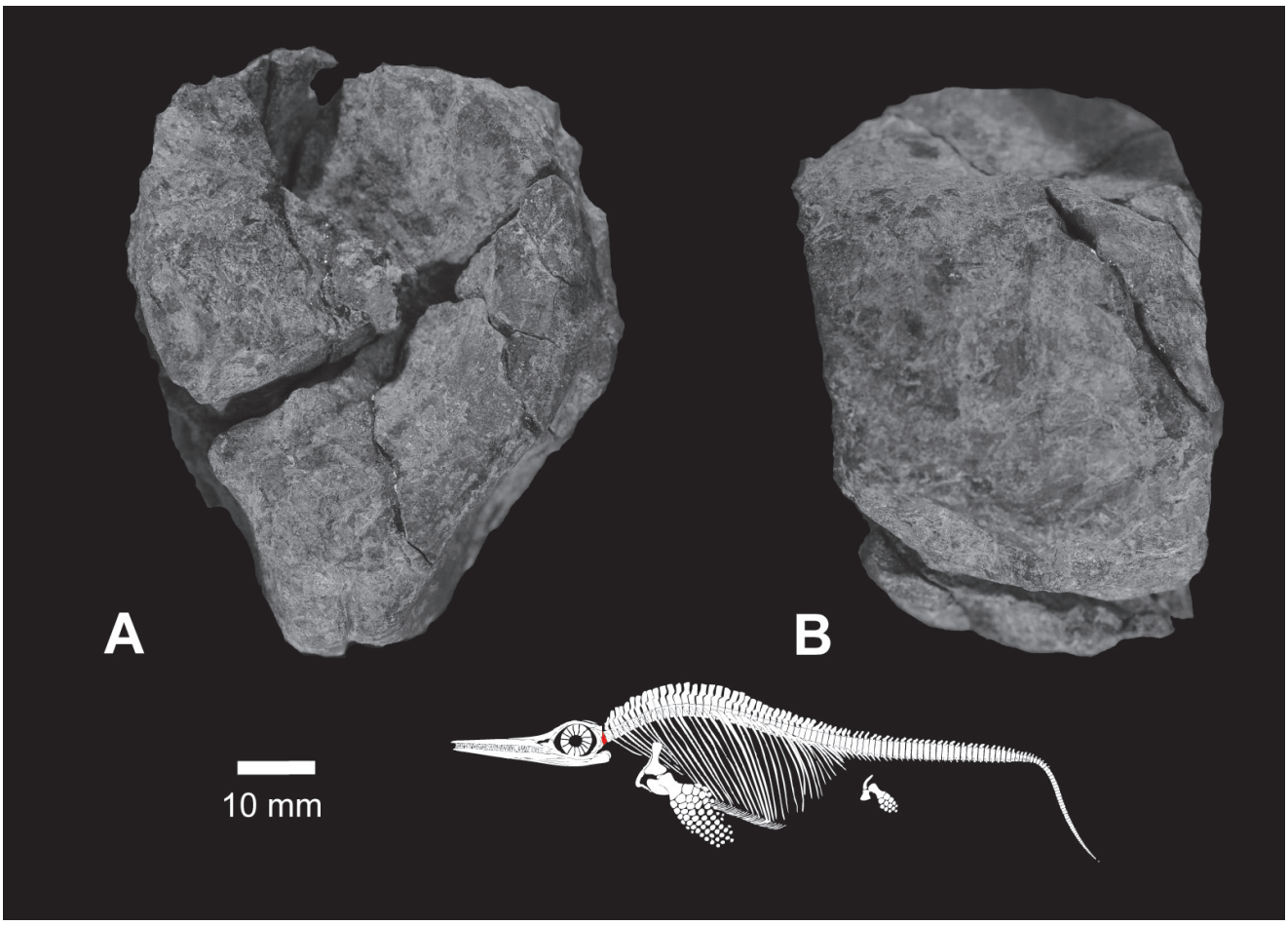

Figure 20. Atlas-axis complex of Palvennia hoybergeti, *SVB 1451, in posterior (A) and right-lateral (B) views.*

Postcranium

A partial atlas-axis complex is preserved in SVB 1451, but is incomplete and poorly preserved (Figure 20). The atlas and axis are fused; although the line of fusion can be clearly seen along the lateral surface, no indication of apophyses can be discerned. The complex is 52 mm in anteroposterior length along the lateral surface and has a maximum mediolateral width of 55 mm. Both articular surfaces are strongly concave. In articular view, the complex is taller than wide and is shaped like an inverted triangle in outline, with the ventral margin forming a broad and prominent keel that bears a narrow trough along its ventral midline.

Only fragmentary portions of the forefin are present. The only clearly identifiable element is a small portion of the distal end of what is interpreted to be the humerus based on overall size (Figure 21). This fragment preserves a small, but complete facet along one edge. The size and location of the facet strongly suggests that it is neither the radial or ulnar facet. It is therefore most probable that it is the facet for an accessory element, likely the preaxial accessory element, consistent with it being an ophthalmosaurid.

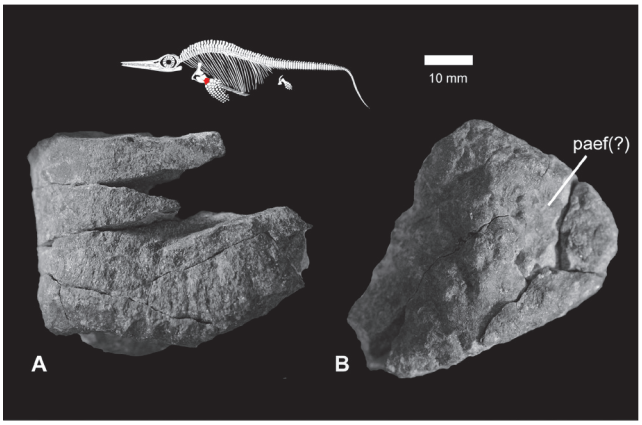

Figure 21. Fragment of the distal end of the humerus of Palvennia hoybergeti, *SVB 1451, in dorsal? (A) and distal (B) views. Abbreviation: paef, postaxial accessory element facet.*

Discussion

Comparisons of Cryopterygius *with other ophthalmosaurids*

Cryopterygius (PMO 214.578) can be confidently referred to Ophthalmosauridae on the basis of possessing a preaxial accessory element in the zeugopodial row and a reduced extracondylar area of the basioccipital (as noted at the time of collection but currently situated on the unprepared side of the specimen and not visible). *Cryopterygius* is therefore compared to other well-known ophthalmosaurids including *Ophthalmosaurus icenicus* Seeley, 1874 from the Oxford Clay Formation (Callovian), *Brachypterygius extremus* (Boulenger, 1904) and *Nannopterygius enthekiodon* (Hulke, 1871) from the Kimmeridge Clay Formation (Kimmeridgian-Tithonian), *Undorosaurus gorodischensis* Efimov, 1999b from Russia (Volgian), *Caypullisaurus bonapartei* Fernández, 1997 from the Vaca Muerta Formation (Tithonian), A*rthropterygius chrisorum* (Russell, 1993) from the Ringnes Formation (Oxfordian to Kimmeridgian) and *Aegirosaurus leptospondylus* (Wagner, 1853) from the Solnhofen Formation (Tithonian), as well as Lower Cretaceous forms including *Acamptonectes* Fischer *et al.*, 2012 (Hauterivian), *Sveltonectes* Fischer *et al.*, 2011 (Barremian), *Athabascasaurus* Druckenmiller & Maxwell, 2010 (Albian) and various species of *Platypterygius* Huene, 1922.

In the proportions of its rostrum, the holotype specimen of *Cryopterygius* (PMO 214.578) is relatively shorter than *Nannopterygius*, *Ophthalmosaurus icenicus* and *Aegirosaurus* (Kirton, 1983; Bardet & Fernández, 2000), but is more robust and most similar to *Brachypterygius extremus* (McGowan, 1976; CAMSM J68516) in this regard. On the basis of orbital ratios, the orbit of *Cryopterygius* is somewhat larger than *B. extremus*, but relatively smaller than *O. icenicus* or *Nannopterygius* (Kirton, 1983). The premaxilla of *Cryopterygius* is most similar to *O. icenicus* in possessing a reduced supranarial process that is shorter than the subnarial process and that does not contact the external naris, unlike the condition seen in *Platypterygius americanus*, *B. extremus*, and *Caypullisaurus* (Romer, 1968; Kirton, 1983; Fernández, 1997). The subnarial process is also very distinct from that of *B. extremus*, in which the latter shares a broad contact with the jugal. A lacrimal-external naris contact is absent in PMO 214.578 (likely separated by a posterior ascending process of the maxilla), similar to *Platypterygius australis* and *Athabascasaurus* (Kear, 2005; Druckenmiller & Maxwell, 2010), but different from *O. icenicus*, *Aegirosaurus*, *Caypullisaurus* and *Sveltonectes* (Kirton, 1983; Bardet & Fernández, 2000; Fernández, 2007; Fischer *et al.*, 2011). The lacrimal in *Cryopterygius* is also distinct in possessing a well-defined, 90-degree bend along its posterior margin, unlike the more gently curving condition seen in well preserved specimens of ophthalmosaurids, including *Ophthalmosaurus* and *P. australis* (Kirton, 1983; Kear, 2005). The maxilla of *Cryopterygius* exhibits a much greater lateral exposure along the toothrow compared to *Aegirosaurus*, *Sveltonectes* and *O. icenicus* and is more similar to *Caypullisaurus* in that the maxilla terminates far posteriorly, nearly as far as the midpoint of the orbit. However, the high maxillary tooth count (23) is nearly identical to *B. extremus*. The jugal is also similar to *B. extremus* in being relatively straight, but differs markedly from the bowed condition seen in *Aegirosaurus*, *O. icenicus* and *P. australis*.

The morphology of the postorbital bar in *Cryopterygius* is unique. The bar is conspicuously broad, similar to

Platypterygius americanus and *Caypullisaurus* (Romer, 1968; Fernández, 1997), but unlike the narrow condition observed in *Aegirosaurus*, *Ophthalmosaurus icenicus* or *Nannopterygius* (Andrews, 1910; Bardet & Fernández, 2000; Kirton, 1983). However, the presence of an unidentified element (likely the supratemporal) lying posterior to the quadratojugal and projecting ventrally as a process into the posteroventral area of the cheek region is likely autapomorphic for *Cryopterygius*, as it has not been described in any other ophthalmosaurid. In terms of its dentition, PMO 214.578 possesses a tooth count in its upper tooth row (53) nearly identical to *Brachypterygius extremus*, but much larger than that of *Ophthalmosaurus* (40; Kirton, 1983). The teeth are also relatively robust, similar to that of *B. extremus* (tooth length index 0.20; Kirton, 1983), in contrast to the relatively smaller dentition of *Palvennia*, *Aegirosaurus* and *Sveltonectes* (Bardet & Fernández, 2000; Fischer *et al.,* 2011).

Cryopterygius possesses a relatively high number (52) of presacral vertebrae, the same as *Aegirosaurus*, similar to *Caypullisaurus* (50), and slightly less than that estimated for *Platypterygius playtydactylus* (54; Broili, 1907). In contrast, this count is significantly greater than that observed in typical Lower Jurassic taxa (approximately 45; McGowan & Motani, 2003), *Ophthalmosaurus icenicus* (42-43; Kirton, 1983), *Athabascasaurus* (42; Druckenmiller & Maxwell, 2010), and the estimated 37 presacrals in *Platypterygius americanus* (Nace, 1939). Because the vertebrae remain in articulation, comparative comments on centrum morphology are not possible.

The neural spine morphology is distinctive in possessing a conspicuous V-shaped apical notch in the neural spines in lateral view throughout the presacral series. An identical feature has also been described in the neural spines of vertebrae 11 to 20 (more posterior spines were not completely preserved) of *Platypterygius australis* (Wade, 1990). Andrews (1910) and Kirton (1983) note the presence of a shallow groove along the dorsal surface of the spine in *Ophthalmosaurus icenicus*, and a concave and pitted surface has been reported in *Acamptonectes* (Fischer *et al.*, 2012), presumably for reception of a soft tissue cap. The notched apical ends of *Cryopterygius* may have served as sites for attachment of a median ligament, *ligamentum nuchae*, as has been inferred in other diapsids (Tsuihiji, 2004). Alternatively, Wade (1990) suggested that they provided adhesive surfaces for median cartilages supporting a dorsal fin similar to that seen in *Stenopterygius* or *Orca*. However, given that the notches are present throughout the entire presacral series in PMO 214.578 (and that their complete extent in the vertebral column of in *P. australis* is unknown), their association with a *Stenopterygius* or delphinid-like dorsal fin is improbable.

The forelimb of PMO 214.578 is easily distinguished from nearly all other Middle to Late Jurassic ophthalmosaurids in possessing a relatively small paddle with only five (or possibly six) digits and a reduced number of phalanges (Figure 22). The low but robust dorsal process of *Cryopterygius* differs from the tall and narrow morphology seen in the humerus of *Sveltonectes*, *Acamptonectes* and many species of *Platypterygius* (Fischer *et al.,* 2011; Fischer *et al.,* 2012). Notably, the humerus of *Cryopterygius* bears only two, major, distal articular facets for the radius and ulna (Figure 22), although a very diminutive third facet is present anteriorly on the right humerus. In contrast, *Ophthalmosaurus icenicus*, *Brachypterygius extremus*, *Caypullisaurus*, *Undorosaurus gorodischensis*, *Aegirosaurus* and *Acamptonectes* all bear three well developed facets on the distal end of their humeri for either the intermedium or a preaxial accessory element (Boulenger, 1904; Kirton, 1983; Fernández, 1997; Efimov, 1999b; Bardet & Fernández, 2000, Fischer *et al.,* 2012). In *Nannopterygius* (Kirton, 1983) and *Sveltonectes* (Fischer *et al.*, 2011), the distal end of the humerus also bears only two facets. Similarly, the relative size of the humeri in both *Cryopterygius* and *Nannopterygius* are small, having a humerus to jaw length ratio of 0.112 and 0.116, respectively (Kirton, 1983). Unfortunately, other details of the limb in *Nannopterygius* are lacking, including the number of digits, the morphology of the humerus, and the presence and shape of a preaxial accessory element. Interestingly, PMO 214.578 also resembles the Albian taxon *Platypterygius americanus* (UW 2421) in its humeral and zeugopodial morphology (Maxwell & Kear, 2010); however, while a complete forelimb for this taxon is unknown, it does possess associated rectangular phalanges typical of this genus, in contrast to the more rounded phalanges of *Cryopterygius*.

In overall limb and humeral morphology, *Cryopterygius* most closely resembles that of the poorly known Russian taxon *Undorosaurus* (Efimov, 1999b). While *Undorosaurus* possesses a third facet for articulation with the preaxial accessory element, this articular surface is small and approaches the size of the diminutive facet seen in the right humerus of PMO 214.578, suggesting that some degree of morphological plasticity is present in this feature. However, *Undorosaurus* bears five digits in total, while there are possibly six in *Cryopterygius*. Also, both taxa differ somewhat in the morphology of the radius and ulna, the proximal carpals and particularly in the shape of the preaxial accessory element. It is noteworthy that another specimen (BNSS 0006) from the Oxford Clay Formation of the UK (Dorset) also bears a similar overall morphology to *Undorosaurus*, suggesting that this general forelimb morphotype may be more common that has been previously recognised (Delair, 1987).

The wide range of intraspecific variation in the pectoral girdle of ophthalmosaurids (Maxwell & Druckenmiller, 2011) makes it difficult to draw many taxonomically meaningful conclusions between *Cryopterygius* and other comparators; however, some broad comparisons can be made. In their general morphology, the scapula and coracoid of *Cryopterygius* fall within the

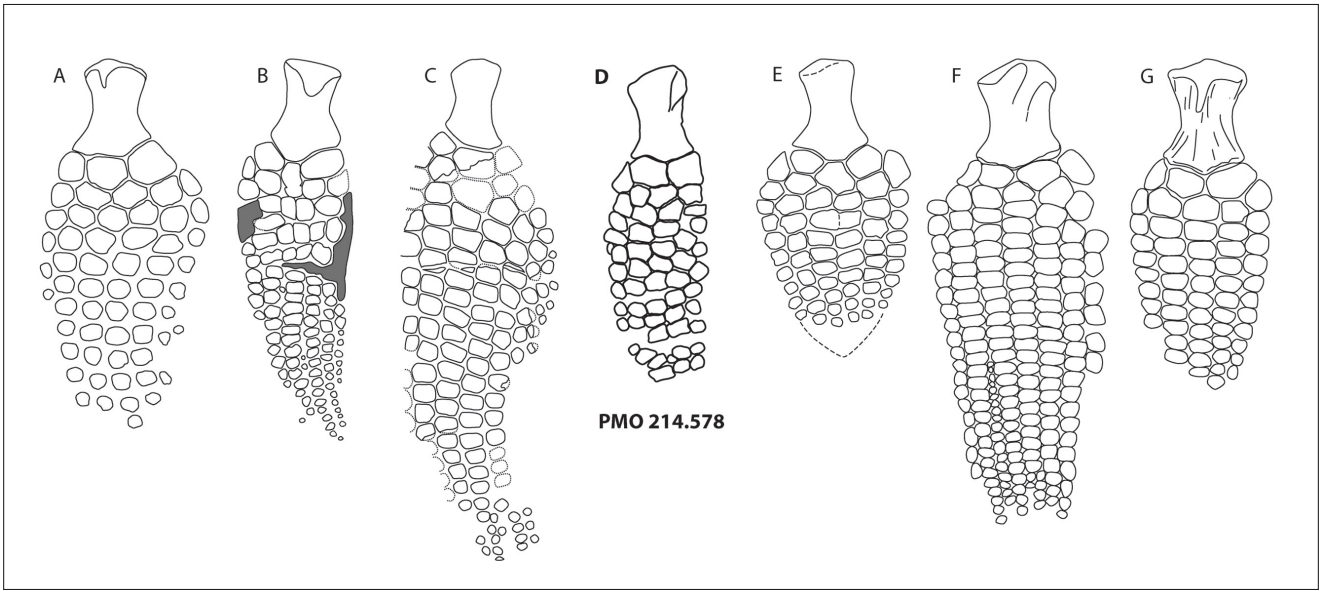

Figure 22. Comparison of left forelimb morphology of selected ophthalmosaurids in dorsal view: A, Ophthalmosaurus icenicus*; *B,* Aegirosaurus leptospondylus*; *C,* Caypullisaurus bonapartei*; D,* Cryopterygius kristiansenae *(in bold); E,* Brachypterygius extremus*; *F,* Platypterygius hercynicus*; *G,* Undorosaurus 'nessovi' *c.f.* gorodischensis*. *Redrafted from A, Kirton (1983); B, Bardet & Fernández (2000); C, Fernández (1997); E, Boulenger (1904); F, Kolb & Sander (2009); G, Efimov (1999b). *mirrored from right limb.*

range of variation observed in *Ophthalmosaurus icenicus* (Kirton, 1983) and are also broadly similar to that of *Undorosaurus* sp. (Efimov, 1999b). The pectoral girdle of *Caypullisaurus* is incompletely known, but the scapular blade is relatively longer than that of PMO 214.578. The pectoral girdles figured for '*Yasykovia*' (Efimov, 1999a; likely a junior synonym of *Ophthalmosaurus*; McGowan & Motani, 2003) differs from *Cryopterygius*, particularly in the coracoids being much anteroposteriorly longer than broad, and the very well developed anterior portion of the scapula, which actually forms a distinct facet for a bone-to-bone contact with the coracoid in *Y. "kabanovi"* (Efimov, 1999a). The overall scapular morphology of *Platypterygius americanus* also differs in that the scapula is nearly bilaterally symmetrical in lateral view along its anteroposterior axis (Maxwell & Kear, 2010), whereas the scapular blade is located relatively more anteriorly with respect to the proximal end of the bone in *Cryopterygius*, and most other Late Jurassic ophthalmosaurids. The coracoids of *Nannopterygius* are much smaller compared to the overall body size of *Cryopterygius*, although other details of their morphology remain poorly known (Hulke, 1871). The coracoid of *P. australis* is also more rounded in outline than *Cryopterygius* and has a very weakly developed anterior process and anterior notch (Zammit *et al.*, 2010).

The pelvic girdle of most ophthalmosaurids is poorly known. With respect to the ilium, comparative material of both *Ophthalmosaurus icenicus* and *Aegirosaurus* differs markedly from *Cryopterygius* in being more rod-like and more strongly curved at its midshaft (Andrews, 1910; Bardet & Fernández, 2000). The ischiopubis of *O. icenicus* also differs from *Cryopterygius* in being less anteroposteriorly expanded distally, possessing a small ischiopubic foramen approximately midway along the shaft, and in the fusion of the pubis and ischium distally (Kirton, 1983). In overall morphology, the ischiopubis of PMO 214.578 most closely resembles that of *Undorosaurus* and material referred to *Ophthalmosaurus* sp. from the Tithonian of France (Bardet *et al.*, 1997), both of which share the same general morphology of a distally expanded, blade-like end. In *Undorosaurus*, the distal end of the pubis is also free and not fused to the ischium, creating a conspicuous notch like that in *Cryopterygius*, while the Tithonian material of *Ophthalmosaurus* sp. from France has a distinct foramen and a distally fused pubis (Bardet *et al.*, 1997).

Compared to other Middle Jurassic to Early Cretaceous taxa, the femur of *Cryopterygius* possesses a unique combination of characters in having a relatively anteroposteriorly expanded distal end, two distal facets, and probably three digits. By comparison, the proximal and distal ends are subequal in width in *Aegirosaurus*, *Ophthalmosaurus icenicus*, *Arthropterygius*, *Caypullisaurus* and *Undorosaurus* (Andrews, 1910; Fernández, 1997; Efimov, 1999b; Maxwell, 2010) and three well-formed distal facets are present in *Platypterygius australis*, *Platypterygius americanus* and '*Yasykovia*' (Maxwell & Kear, 2010; Zammit *et al.,* 2010). The presence of three probable digits differs from 5 in *Caypullisaurus* and *Sveltonectes*, and at least 4 in *Aegirosaurus* (Fernández, 2007; Fischer *et al.,* 2011). A small, partially articulated hind limb referred to *Nannopterygius* from the Kimmeridge Clay Formation (NHMUK 46497) bears a broad

similarity to that of PMO 214.578, but differs in not being as distally expanded and in the shape of the tibia and fibula.

In sum, *Cryopterygius* can be distinguished from other Middle to Late Jurassic ophthalmosaurs on the basis of its cranial morphology. Based on limb morphology, particularly its humerus and ischiopubis, *Cryopterygius* is most similar to *Undorosaurus* from approximately coeval strata (Volgian/Tithonian) of Russia (Efimov, 1999b). However, given other morphological differences between the two taxa, that the skull of *Undorosaurus* is largely unknown, and in light of questions regarding the taxonomic validity of *Undorosaurus*, PMO 214.578 is referred to the new taxon *Cryopterygius* pending the availability of new data.

Comparison of Palvennia with other ichthyosaurs

The rostral index of *Palvennia* is relatively low, indicating a relatively short rostrum compared to *Cryopterygius* and other Middle to Late Jurassic taxa for which these data are available. The rostrum of *Palvennia* is also comparatively more robust than the gracile morphology of *Aegirosaurus* (Bardet & Fernández, 2000). Although the dimensions are approximate, SVB 1451 clearly has a proportionately very large orbit, much larger than *Cryopterygius* (0.19) and more similar to *Ophthalmosaurus* (0.27; Kirton, 1983) and the upper range for *Aegirosaurus* (0.26; Bardet & Fernández, 2000). The maxilla is moderately well exposed laterally along the toothrow, being proportionately longer than *Ophthalmosaurus icenicus* and *Aegirosaurus* (Kirton, 1983; Bardet & Fernández, 2000), but shorter than *Cryopterygius* or *Caypullisaurus* (Fernández, 2007). The maxilla in *Cryopterygius* and *Caypullisaurus* also terminates farther posteriorly, closer to the midpoint of the orbit, than in *Palvennia*. The gently curving posterior margin of the lacrimal in *Palvennia* differs from the condition seen in *Cryopterygius*, which has a distinct 90-degree kink in this area. The jugal of *Palvennia* is strongly bowed, possibly a reflection of the large orbital size in this taxon compared to the straighter morphology of *Cryopterygius* and *Brachypterygius extremus* (Kirton, 1983). The postorbital bar is conspicuously narrow when compared to *Cryopterygius*, *Caypullisaurus* and *Platypterygius americanus* (Romer, 1968), and more closely resembles *O. icenicus* and probably *Nannopterygius* in this regard (Kirton, 1983).

It is not possible to compare the relationships of bones on the skull roof to most taxa because many specimens are laterally compressed. The frontals of *Palvennia* are mediolaterally broad, in contrast to *Ophthalmosaurus icenicus* (Kirton, 1983) and *Athabascasaurus* (Druckenmiller & Maxwell, 2010). In this respect, *Palvennia* is similar to *Platypterygius australis* and *Sveltonectes* (Kear, 2005; Fischer *et al.,* 2011), but in contrast, the frontals of *Palvennia* do not form a considerable portion of the anteromedial wall of the supratemporal fenestra. *Palvennia* also has a broad postfrontal-frontal contact, which is seen in *Athabascasaurus* but not in *P. australis* or *O. icenicus* (Kirton, 1983; Kear, 2005; Druckenmiller & Maxwell, 2010). Most unique in *Palvennia* is the conspicuously large pineal foramen, which is not seen in any other ophthalmosaurid for which material is available.

In posterior articular view the basioccipital of *Palvennia* is nearly oval in outline with only the condyle visible, more similar to *Arthropterygius* (Maxwell, 2010) and *Platypterygius australis* (Kear, 2005). In contrast, the basioccipital of *Ophthalmosaurus icenicus* has a broad extracondylar area visible extending laterally from the condyle (producing a ventral notch in profile; Kirton, 1983; pers. obs. Druckenmiller), whereas in *Brachypterygius extremus* and *Sveltonectes* the basioccipital is much broader in its dorsal half (McGowan, 1976; Fischer *et al.,* 2011). *Brachypterygius* and *Acamptonectes* also differ from *Palvennia* in possessing a dorsally-situated notochordal pit on the occipital condyle, although the taxonomic validity of this feature is unclear (McGowan, 1976; Fischer *et al.,* 2012). In lateral profile, the basioccipital of *Palvennia* resembles *B. extremus* in its general shape; however, *B. extremus*, as well as *Sveltonectes* and *Arthropterygius*, have a very reduced extracondylar area (McGowan, 1976; Maxwell, 2010; Fischer *et al.,* 2011). The relatively broad extracondylar area in *Palvennia* is, in this respect, most similar to that seen in *O. icenicus* and *Acamptonectes* (Kirton, 1983; Fischer *et al.,* 2012). In *Arthropterygius*, the anterior face of the basioccipital possesses a notochordal pit and a distinct basioccipital peg, both of which are absent in *Palvennia* (Maxwell, 2010).

The exoccipital of *Brachypterygius extremus*, *Ophthalmosaurus icenicus*, *Platypterygius australis* and *Acamptonectes* all possess a triangular outline and an anteriorly elongate basioccipital facet (McGowan, 1976; Kirton, 1983; Kear, 2005; Fischer *et al.,* 2012) in contrast to that seen in *Palvennia*. In *B. extremus*, *O. icenicus* and *P. australis* the lateral wall of the exoccipital is perforated by one to three foramina (McGowan, 1976; Kirton, 1983; Kear, 2005), which are also absent in *Palvennia*. The supraoccipital of *O. icenicus* differs in overall morphology from *Palvennia*, especially in having a much smaller and narrower dorsal margin of the foramen magnum and in possessing a pair of conspicuous foramina (pers. obs. Druckenmiller). The stapes of *P. australis* is relatively massive compared to *Palvennia* (Kear, 2005), and in both *O. icenicus* and *P. australis* the stapedial shaft is stouter and lacks the prominent midshaft constriction that is seen in *Palvennia*. The stapes of *Palvennia* is most similar to that of *Acamptonectes* in possessing a relatively gracile stapedial shaft, although the shapes of the opishthotic and basioccipital/basisphenoid facets differ (Fischer *et al.*, 2012).

The small amount of postcranial material limits the number of comparative comments. The atlas axis of *Palvennia* differs from the anteroposteriorly shortened

complex in *Undorosaurus* (Efimov, 1999b). The fragmentary humerus possesses what is interpreted to be a small, third facet for the preaxial accessory element, and in this regard it clearly differs from *Nannopterygius* and *Cryopterygius*, which bear only two distal facets (Kirton, 1983).

Conclusions

New discoveries of ichthyosaurian material from Svalbard, including the exceptionally well preserved holotype specimen of *Cryopterygius*, significantly expand our knowledge of the diversity and distribution of ophthalmosaurids during the latest Jurassic. Ongoing work in the Slottsmøya Member Lagerstätte reveals an ever-expanding diversity during the Volgian/Tithonian interval, particularly in high paleolatitudes. As such, these new finds will constitute important new data points in comparative anatomical, phylogenetic and paleoecological studies of Jurassic ichthyosaurs. Finally, exemplars such as PMO 214.578 and SVB 1451 provide important comparative data for other poorly known Tithonian material from Mexico (Buchy & Olivia, 2009; Buchy, 2010), France (Bardet *et al.*, 1997), Germany (Bardet & Fernández, 2000), Russia (Arkhangelsky, 1997; Arkhangelsky, 2000; Efimov, 1999a; 1999b) and Svalbard (Angst *et al.*, 2010)

Acknowledgements – We offer our hearty thanks to the many people who assisted in the discovery, excavation and preparation of marine reptiles from Svalbard including Ø. Enger, M.-L. and B. Funke, M. Høyberget, L. Kristiansen, S. Larsen, L. Liebe, B. Lund, L. Novis, J. Rousseau, N.S. Munthe-Kaas, N.L. Hernes, and T. Wensås. We thank H.T. and R. Schassberger, H.S. and J.K. Druckenmiller, E. Maxwell, and M. Zammit, M. Fernández, and V. Fischer; and P. Folkesson (3DScanners AB) and P.-E. Bolstad (PreciTech AS) for assistance with laser scanning. H. Foss provided valuable assistance on many of the figures. Institutional assistance was provided by S. Chapman. Financial support for this work was contributed by ExxonMobil, Fugro, OMW, Sptisbergen Travel, Powershop, National Geographic (grant number: EC0425_09), Norwegian Polar Institute. Preparation of SVB 1451 was initially started by Clive Coy, financed by PalVenn, who taught the volunteer M.-L. Knudsen Funke the skills to continue the tedious work of saving the fragmented skull (2005-2006). PMO 214.578 was prepared by L. Kristiansen (2009; financed by National Geographic, grant number: EC0435_09). We thank the reviewers E. Maxwell and V. Fischer for their detailed and helpful comments on the manuscript. Finally, we extend our appreciation to the Friends of the Palaeontological Museum in Oslo (PalVenn) whose tenth anniversary led to the excavation of the first Jurassic ichthyosaur on Svalbard in 2004.

References

Andrews, C.W. 1910: *A descriptive catalogue of marine reptiles of the Oxford Clay - Part 1*. London.

Angst, D., Buffetaut, E., Tabouelle, J. & & Tong, H. 2010: An ichthyosaur skull from the Late Jurassic of Svalbard. *Bulletin de la Société Géologique de France 181(5)*, 453-458.

Arkhangelsky, M.S. 1997: On a new ichthyosaurian genus from the lower Volgian substage of the Saratov, Volga Region. *Paleontological Journal 31(1)*, 87-90.

Arkhangelsky, M.S. 2000: On the ichthyosaur *Otschevia* from the Volgian Stage of the Volga River. *Paleontological Journal 34(5)*, 549-552.

Bardet, N., Duffaud, S., Martin, M., Mazin, J.-M., Suberbiola, X.P. & Vidier, J.-P. 1997: Découverte de l'ichthyosaure *Ophthalmosaurus* dans le Tithonien (Jurassique supérieur) du Boulonnais, Nord de la France. *Neues Jahrbuch für Geologie und Paläontologie. Abhandlungen 205(3)*, 339-354.

Bardet, N. & Fernández, M.S. 2000: A new ichthyosaur from the Upper Jurassic lithographic limestones of Bavaria. *Journal of Paleontology 74*, 503-511.

Baur, G. 1887: Über den Ursprung der Extremitäten der Ichthyopterygia. *Jahresberichte und Mitteilungen des Oberrheinischen geologischen Vereines 20*, 17-20.

Birkenmajer, K. 1980: Jurassic-Lower Cretaceous succession at Agardhbukta, east Spitsbergen. *Studia Geologica Polinica 66*, 35-52.

Bjærke, T. 1978: Mesozoic palynology of Svalbard III. Dinoflagellates from the Rurikfjellet Member, Janusfjellet Formation (Lower Cretaceous) of Spitsbergen. *Palynologia, num extraordin 1*, 69-93.

Blainville, H.M.de. 1835: Description de quelques espèces de reptiles de la Californie, précédé de l'analyse d'un système général d'erpétologie et d'amphibiologie. *Nouvelles Annales du Muséum d'Histoire Naturelle, Paris 4*, 233-296.

Boulenger, G.A. 1904: On a new species of ichthyosaur from Bath. *Proceedings of the Zoological Society of London 1904(1)*, 424-426.

Broili, F. 1907: Ein neuer *Ichthyosaurus* aus der norddeutschen Kreide. *Palaeontographica 54*, 139-162.

Buchholtz, E.A. 2001: Swimming styles in Jurassic ichthyosaurs. *Journal of Vertebrate Paleontology 21*, 61-73.

Buchy, M.-C. 2010: First record of *Ophthalmosaurus* (Reptilia: Ichthyosauria) from the Tithonian (Upper Jurassic) of Mexico. *Journal of Paleontology 84(1)*, 149-155.

Buchy, M.-C. & Olivia, J.G.L. 2009: Occurrence of a second ichthyosaur genus (Reptilia: Ichthyosauria) in the Late Jurassic Gulf of Mexico. *Boletin de la Sociedad Geológica Mexicana 61(2)*, 233-238.

Charola, A.E., Pühringer, J., Steiger, M. 2007: Gypsum: a review of its role in the deterioration of building materials. *Environmental Geology 52*, 339-352.

Collingnon, M. & Hammer, O. 2012: Lithostratigraphy and sedimentology of the Slottsmøya Member at Janusfjellet, Spitsbergen: evidence for a condensed section. *Norwegian Journal of Geology 92*, 89-101.

Dallmann, W.K., Major, H., Haremo, P., Andresen, A., Kjærnet, T. & Nøttvedt, A. 2001: Geological map of Svalbard 1:100,000, sheet C9G Adventdalen. With explanatory text. *Norsk Polarinstitutt Temakart 31/32*, 4-55.

Delair, J.B. 1987: An unusual ichthyosaurian forelimb from Rodwell, Dorset. *Proceedings of the Dorset Natural History and Archaeological Society 108*, 210-212.

Druckenmiller, P.S. & Maxwell, E.E. 2010: A new Lower Cretaceous (lower Albian) ichthyosaur from the Clearwater Formation, Alberta, Canada. *Canadian Journal of Earth Sciences 47*, 1037-1053.

Dypvik, H., Nagy, J., Eikeland, T.A., Backer-Owe, K., Andresen, A., Haremo, P., Bjaerke, T., Johansen, H. & Elverhoi, A. 1991a: The Janusfjellet Subgroup (Bathonian to Hauterivian) on central Spitsbergen: a revised lithostratigraphy. *Polar Research 9(1)*, 21-43.

Dypvik, H., Nagy, J., Eikeland, T.A., Backer-Owe, K. & Johansen, H. 1991b: Depositional conditions of the Bathonian to Hauterivian Janusfjellet Subgroup, Spitsbergen. *Sedimentary Geology 72*, 55-78.

Dypvik, H., Hakansson, E. & Heinberg, C. 2002: Jurassic and Cretaceous palaeogeography and stratigraphic comparisons in the North Greeenland-Svalbard region. *Polar Research 21(1)*, 91-108.

Efimov, V.M. 1999a: Ichthyosaurs of a new genus *Yasykovia* from the Upper Jurassic strata of European Russia. *Paleontological Journal 33(1)*, 91-98.

Efimov, V.M. 1999b: A new family of ichthyosaurs, the Undorosauridae fam. nov. from the Volgian Stage of the European part of

Russia. *Paleontological Journal 33*, 174-181.
Ershova, E.S. 1983: Explanatory notes for the biostratigraphical scheme of the Jurassic and Lower Cretaceous deposits of Spitsbergen archipelago. *Leningrad PGO Sevmorgeologia*.
Fernández, M.S. 1997: A new ichthyosaur from the Tithonian (Late Jurassic) of the Neuquén Basin, Northwestern Patagonia, Argentina. *Journal of Paleontology 71(3)*, 479-484.
Fernández, M.S. 2007: Redescription and phylogenetic position of *Caypullisaurus* (Ichthyosauria: Ophthalmosauridae). *Journal of Paleontology 81*, 368-375.
Fischer, V., Masure, E., Arkhangelsky, M.S. & Godefroit, P. 2011. A new Barremian (Early Cretaceous) ichthyosaur from western Russia. *Journal of Vertebrate Paleontology 31*, 1010-1025.
Fischer, V., Maisch, M.W., Naish, D., Liston, J., Kosma, R., Joger, U., Krüger, F.J., Pardo-Pérez, J., Tainsh, J. & Appleby, R.M. 2012: New ophthalmosaurids from the Early Cretaceous of Europe demonstrate extensive ichthyosaur survival across the Jurassic–Cretaceous boundary. *PLoS ONE 7*, e29234.
Gradstein, F.M., Ogg, J., Schmitz, M.A. & Ogg, G. 2012: *A Geologic Time Scale 2012*. Elsevier Publishing Company.
Hammer, O., Nakrem, H.A., Little, C.S.T., Hryniewicz, K., Sandy, M.R., Hurum, J.H., Druckenmiller, P.S., Knutsen, E.M. & Høyberget, M. 2011: Hydrocarbon seeps close to the Jurassic-Cretaceous boundary, Svalbard. *Palaeogeography, Palaeoclimatology, Palaeoecology 306*, 15-26.
Heintz, N. 1964: Mesozoic reptiles from Norway and Svalbard. *Norsk Polarinstitutt Meddelelser 19*, 1-39.
Huene, F.v. 1922: *Die Ichthyosaurier des Lias und ihre Zusammenhänge*. Verlag von Gebrüder Borntraeger, Berlin.
Hulke, J.W. 1871: Note on an *Ichthyosaurus (I. enthekiodon)* from Kimmeridge Bay, Dorset. *Quarterly Journal of the Geological Society of London 27*, 440-441.
Hurum, J.H., Nakrem, H.A., Hammer, Ø, Knutsen, E.M., Druckenmiller, P.S., Hryniewicz, K. & Novis, L.K. 2012: An Arctic Lagerstätte – the Slottsmøya Member of the Agardhfjellet Formation (Upper Jurassic – Lower Cretaceous) of Spitsbergen. *Norwegian Journal of Geology 92*, 55-64.
Johnson, R. 1977: Size independent criteria for estimating relative age and the relationship among growth parameters in a group of fossil reptiles (Reptilia: Ichthyosauria). *Canadian Journal of Earth Sciences 14*, 1916-1924.
Kear, B.P. 2005: Cranial morphology of *Platypterygius longmani* Wade, 1990 (Reptilia: Ichthyosauria) from the Lower Cretaceous of Australia. *Zoological Journal of the Linnean Society 145*, 583-622.
Kirton, A.M. 1983: *A review of British Upper Jurassic ichthyosaur*s. Ph.D. Dissertation, University of Newcastle upon Tyne, Newcastle upon Tyne.
Kolb, C. & Sander, P.M. 2009: Redescription of the ichthyosaur *Platypterygius hercynicus* (Kuhn 1946) from the Lower Cretaceous of Salzgitter (Lower Saxony, Germany). *Palaeontographica, Abteilung A 288*, 151-192.
Løfaldi, M. & Thusu, B. 1976: Microfossils from the Janusfjellet Subgroup (Jurassic-Lower Cretaceous) at Agardhfjellet and Keilhausfjellet, Spitsbergen. A preliminary report. *Norsk Polaristitutet Årbok*, 125-136.
Maisch, M.W. 2010: Phylogeny, systematics, and origin of the Ichthyosauria – the state of the art. *Palaeodiversity 3*, 151–214.
Maxwell, E.E. 2010: Generic reassignment of an ichthyosaur from the Queen Elizabeth Islands, Northwest Territories, Canada. *Journal of Vertebrate Paleontology 30(2)*, 403-415.
Maxwell, E.E. & Kear, B.P. 2010: Postcranial anatomy of *Platypterygius americanus* (Reptilia: Ichthyosauria) from the Cretaceous of Wyoming. *Journal of Vertebrate Paleontology 30(4)*, 1059-1068.
Maxwell, E.E. & Druckenmiller, P.S. 2011: A small ichthyosaur from the Clearwater Formation (Alberta, Canada) and a discussion of the taxonomic utility of the pectoral girdle. *Paläontologishe Zeitschrift 85(4)*, 457-463.
Maxwell, E.E., Zammit, M. & Druckenmiller, P.S. 2012. Morphology and orientation of the ichthyosaurian femur. *Journal of Vertebrate Paleontology 32(5)*, 1207-1211.
McGowan, C. 1974: A revision of the longipinnate ichthyosaurs of the Lower Jurassic of England, with descriptions of two new species (Reptilia: Ichthyosauria). *Life Sciences Contributions, Royal Ontario Museum 97*, 1-37.
McGowan, C. 1976: The description and phenetic relationships of a new ichthyosaur genus from the Upper Jurassic of England. *Canadian Journal of Earth Sciences 13*, 668-683.
McGowan, C. & Motani, R. 2003: Ichthyopterygia. *In* Sues, H.D. (ed.): *Handbook of Paleoherpetology, Part 8*. Verlag Dr. Friedrich Pfeil, München.
Motani, R. 1999: On the evolution and homologies of ichthyopterygian forefins. *Journal of Vertebrate Paleontology 19*, 28-41.
Nace, R.L. 1939: A new ichthyosaur from the Upper Cretaceous Mowry Formation of Wyoming. *American Journal of Science 237*, 673-686.
Nagy, J. & Basov, V.A. 1998: Revised foraminferal taxa and biostratigraphy of Bathonian to Ryazanian deposits in Spitsbergen. *Micropaleontology 44*, 217-255.
Ogg, J. 2004: The Jurassic Period. *In* Gradstein, F.M., Ogg, J. & Smith, A. (eds.): *A geologic time scale 2004*, 307-343. Oxford University Press.
Parker, J.R. 1976: The Jurassic and Cretaceous sequence in Spitsbergen. *Geological Magazine 104*, 487-505.
Persson, P.O. 1962: Plesiosaurians from Spitsbergen. *Norsk Polarinstitutt 1962*, 62-68.
Romer, A.S. 1968: An ichthyosaur skull from the Cretaceous of Wyoming. *Contributions to Geology 7*, 27-41.
Russell, D.A. 1993: Jurassic marine reptiles from Cape Grassy, Melville Island, Arctic Canada; pp. 195-201 *in* Christie, R.L. & McMillan, N.J. (eds.), *The Geology of Melville Island, Arctic Canada*. Geological Survey of Canada Bulletin 450.
Seeley, H.G. 1874: On the pectoral arch and forelimb of *Ophthalmosaurus*, a new ichthyosaurian genus from the Oxford Clay. *Quarterly Journal of the Geological Society of London 30*, 696-707.
Tsuihiji, T. 2004: The ligament system in the neck of *Rhea americana* and its implication for the bifurcated neural spines of sauropod dinosaurs. *Journal of Vertebrate Paleontology 24*, 165-172.
Wade, M. 1990: A review of the Australian Cretaceous longipinnate ichthyosaur *Platypterygius*, (Ichthyosauria, Ichthyopterygia). *Memoirs of the Queensland Museum 28(1)*, 115-137.
Wagner, A. 1853: Die Characteristic einer neuen Art von *Ichthyosaurus* aus den lithographischen Schiefern und eines Zahnes von *Polyptychodon* aus dem Gründsansteine von Kelheim. *Bulletin der königlische Akademie der Wissenschaft, Gelehrte Anzeigen 3*, 25-35.
Wiman, C. 1914: Ein Plesiosaurierwirbel aus dem jüngeren Mesozoicum Spitzbergens. *Bulletin - Uppsala Universiteter, Mineralogisk-geologiska Institut 12*, 201-204.
Wierzbowski, A., Hryniewicz, K., Hammer, Ø., Nakrem, H.A. & Little, C.T.S. 2011: Ammonites from hydrocarbon seep carbonate bodies from the uppermost Jurassic–lowermost Cretaceous of Spitsbergen, Svalbard, and their biostratigraphic importance. *Neues Jahrbuch für Geologie und Paläontologie Abhandlungen 262*, 267–288.
Zammit, M., Norris, R. & Kear, B.P. 2010: The Australian Cretaceous ichthyosaur *Platypterygius australis*: a description and review of postcranial remains. *Journal of Vertebrate Paleontology 30(6)*, 1726-1735.